INTERNATIONAL ATOMIC ENERGY AGENCY
INTERNATIONAL CENTRE FOR THEORETICAL PHYSICS
I.C.T.P., P.O. BOX 586, 34100 TRIESTE, ITALY, CABLE: CENTRATOM TRIESTE

SMR.1065 - 4

COLLEGE ON SOIL PHYSICS
14 - 30 APRIL 1998

"Water Balance"
"Electromagnetic Wave Attenuation in Soil Physics"
"Neutron Probes and their Use in Agronomy"

Klaus REICHARDT
Escola Superior de Agricultura 'Luiz de Queiroz' (ESALQ)
Universidade de Sao Paulo (USP)
Departmento de Solos
Av. Padua Dias 11
Caixa Postal 9
13418-900 Piracicaba
BRAZIL

These are preliminary lecture notes, intended only for distribution to participants

WATER BALANCE

K. Reichardt[1,2,4], O.O.S. Bacchi[2,4], J.C.M. Oliveira[2,5], D. Dourado - Neto[3,4], J.E. Pilotto[2]

1. Introduction

The intense water cycling in a watershed or in a cropped field can be characterized and quantified in making a water balance, which is the computation of all water fluxes at the boundaries of the system under consideration. It is an itemized statement of all gains, losses and changes of storage of water, within a specified volume element soil. Its knowledge is of extreme importance for the correct management of water in natural and agro-systems. It gives an indication of the strength of each component, which is important for their control and to ensure the utmost productivity with a minimum interference in the environment.

2. Volume Element and Components

Considering the whole physical environment of a field crop, a volume element of soil is defined to establish the balance, having an unit area (1 m^2), ranging from the soil surface ($z = 0$) to the bottom of the root zone ($z = L$), where z (m) is the vertical position coordinate. Water fluxes are considered only in the z direction, with exception to the runoff. It is, therefore, an unidirectional approach, which is a simplification that is best valid within the soil, when fairly homogeneous.

Water fluxes are actually water flux densities, which correspond to amounts of water that flow per unit of cros-sectional area and per unit of time. One convenient unit is liters of water per square meter per day, which corresponds to $mm.day^{-1}$. They are vectors, assumed positive when entering the volume element (gain), and negative when leaving (loss).

[1] Department of Physics and Meteorology, ESALQ/USP, C.P. 9, 13418-900, Piracicaba, SP, Brazil.
[2] Soil Physics Laboratory, CENA, USP, C.P. 96, 13418-970, Piracicaba, SP, Brazil.
[3] Department of Agronomy, ESALQ/USP, C.P. 9, 13418-900, Piracicaba, SP, Brazil.
[4] CNPq fellow
[5] FAPESP fellow

At the upper boundary, the soil surface (z = 0), rainfall (**p**) and irrigation (**i**) are considered gains; evaporation (**e**), transpiration (**t**), or evapotranspiration (**et**), are losses, and the runoff (**r**) can be either a loss or a gain, depending on the water flow being into or out of the area considered for the balance.

At the lower boundary, the bottom of the root zone (z = L), soil water fluxes ($\mathbf{q}_L$) can be gains or losses depending on their sense (upward or downward).

Figure 1 is a schematic view of the volume element and of the fluxes that compose the balance.

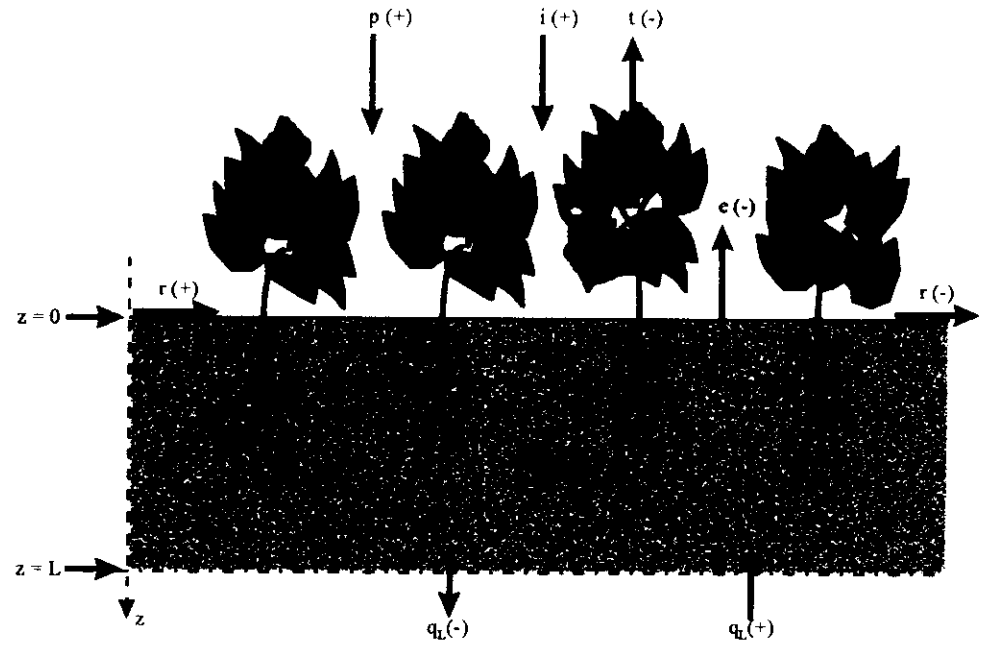

3. The Balance

The balance is an expression of the mass conservation law, which can be written for the elemental volume as follows:

$$\sum \mathbf{f} = \int_0^L \frac{\partial \theta}{\partial t} dz \quad \text{.....(1)}$$

where θ is the soil water content ($m^3.m^{-3}$), t the time (day) and **f** stands for the flux densities **p**, **i**, **t**, **e**, **r** and **q**. The entrance or leave of the fluxes **f** in the elemental volume give rise to changes in soil water contents $\partial\theta/\partial t$, which integrated over the depth interval z = 0 and z = L, represent changes in soil water storage S. Therefore:

$$\mathbf{p} + \mathbf{i} - \mathbf{et} \pm \mathbf{r} \pm \mathbf{q}_L = \frac{\partial S}{\partial t} \quad \text{.....(2)}$$

where S is defined by

$$S = \int_0^L \theta dz \quad \text{.....(3)}$$

Equation (2) is an instantaneous view of the balance. When integrated over a time interval $\Delta t = t_f - t_i$, in days, yields amounts of water (mm):

$$\int_{t_i}^{t_f} (\mathbf{p} + \mathbf{i} - \mathbf{et} \pm \mathbf{r} \pm \mathbf{q}_i) dt = \int_{t_i}^{t_f} \int_0^L \frac{\partial \theta}{\partial t} dz dt \quad \text{.....(4)}$$

or

$$\mathbf{P} + \mathbf{I} - \mathbf{ET} \pm \mathbf{R} \pm \mathbf{Q}_L = \Delta S \quad \text{.....(4a)}$$

When all but one of the above components are known, the unknown is easily calculated algebraically. Five short examples are given below.

1. A soil profile stores 280 mm of water and receives 10 mm of rain and 30 mm of irrigation. It loses 40 mm by evapotranspiration. Neglecting runoff and soil water fluxes below the root zone, what is its new storage?
2. A soybean crop loses 35 mm by evapotranspiration in a period without rainfall and irrigation. It loses 8 mm through deep drainage. What is its change in storage?
3. During a rainy period, a plot receives 56 mm of rain, of which 14 mm are lost by runoff. Deep drainage amounts to 5 mm. Neglecting evapotranspiration, what is the storage change?
4. Calculate the daily evapotranspiration of a bean crop which, in a period of 10 days, received 15 mm of rainfall and two irrigations of 10 mm each. In the same period, the deep drainage was 2 mm and the change in storage - 5 mm.
5. How much water was given to a crop through irrigation, knowing that in a dry period its evapotranspiration was 42 mm and the change in storage was -12 mm? Soil was at field capacity and no runoff occured during irrigation.

SOLUTIONS

n°	P	+	I	-	ET	±RO	$\pm Q_L$	=	ΔS_L	Answer
1	10		30		-40	0	0	=	0	280 mm
2	0		0		-35	0	-8	=	-43	-43 mm
3	56		0		0	-14	-5	=	+37	+37 mm
4	15		20		-38	0	-2	=	-5	-3.8 mm.day^{-1}
5	0		30		-42	0	0	=	-12	+30 mm

The time interval Δt used to integrate equation (z) is the time interval over which the water balance is made. Its choice depends on the objectives of the balance. Intervals shorter than one day are seldomly used. Periods of 3, 7, 10, 15 days are very common, and larger ones are used in environmental studies.

4. Discussion of the Components

4.1 Rainfall

Rainfall is easily measured with simple rain gauges which consist of containers of a cross sectional area A (m^2), which collect a volume ~~rain gauges~~ V(liters) of rain, corresponding to a rainfall depth h(mm) equal to h = V/A. The problem in its measurement lies in its variability in space and time. In the case of whole watersheds, rain gauges have to be well distributed, following a scheme based on rainfall variability data. For the case of small experimental fields, attention must be taken to the distance of the gauge in relation to the water balance plots. Reichardt et al. (1995) is an example of rainfall variability study, carried out in a tropical zone, where localized thunder-storms play an important role.

4.2 Irrigation

The measurement of the irrigation depth that effectively infiltrated into a given soil at a given area is not an easy task. Different methods of irrigation (sprinkler, furrow, drip, flooding, etc...) present great space variabilities which have to be taken into account.

4.3 Evapotranspiration (ET)

Evapotranspiration can be measured independently or estimated from the balance, if all other components are known. In the first case, a great number of reports are found in the literature, covering classical methods like those proposed by Thorthwaite, Braney-Criddle and Penmann, which are based on atmospheric parameters such as air temperature and humidity, wind, solar radiation, etc. These methods have all their own shortcomings, mainly because they

do not take into account plant and soil factors. Several models, however, include aspects of plant and soil, and yield much better results.

The main problem of estimating ET from the balance lies in the separation of the contribution of the components ET and Q_L, since both lead to changes in soil water storage ΔS. One important thing is that the depth L has to be such that it includes the whole root system. If there are roots below z = L, ET is underestimated. If L covers the whole root system and Q_L is well estimated, which is difficult as will be seen below, ET can be estimated from the balance. Villagra et al (1995) discuss these problems in detail.

4.4 Runoff (R)

Runoff is difficult to be estimated since its magnitude depends on the slope of the land, the length of the slope, soil type, soil cover, etc. For very small slopes, runoff is in general neglected. If soil is managed correctly, using contour lines, even with significant slopes runoff can be neglected. In cases it can not be neglected, runoff is measured in ramps, about 20 m long and 2 m wide, covering an area of 40 to 50 m^2, with a water collector at the lower end. Again, the runoff depth h (mm) is the volume V (liters) of the collected water, divided by the area A (m^2) of the ramp. Several reports in the literature cover the measurement of R, and its extrapolation to different situations of soil, slope, cover, etc. This is a subject very well considered in other opportunities of this College.

4.5 Soil Water Fluxes at z = L, Q_L

The estimation of soil water fluxes at the lower boundary z = L, can be estimated using Darcy-Buckingham's equation, integrated over the time:

$$Q_L = \int_{t_i}^{t_f} [K(\theta)\partial H / \partial z]dt \quad \text{.....(5)}$$

where $K(\theta)$, (mm day^{-1}) is the hydraulic conductivity estimated at the depth z = L, and $\partial H/\partial z$ (m m^{-1}) the hydraulic potential head gradient, H (m) being assumed to be the sum of the gravitational potential head z, (m) and the matric potential head h, (m). Therefore it is necessary to measure $K(\theta)$ at z = L and the most common procedures used are those presented by Hillel et al (1972), Libardi et al (1980), and Sisson et al (1980). These methods present several problems, discussed in detail in Reichardt et al (1998). The use of this $K(\theta)$ relations

involves two main constraints: (i.) the strong dependence of K upon θ, which leads to exponential or power models, and (ii.) soil spatial variability.

Common K(θ) relations are:

$$K = K_o \exp\left[\beta(\theta - \theta_o)\right] \quad \text{.....(6)}$$

and

$$K = a\theta^b \quad \text{.....(7)}$$

in which β, a and b are fitting parameters, K_o the saturated hydraulic conductivity, and θ_o the soil water content saturation. Reichardt et al (1993) used model (6), and for 25 observation points of a transect on a homogeneous dark red latosol, obtained an average equation with $\overline{K}_o = 144.38 \pm 35.33$ mm day^{-1}, and $\overline{\beta} = 111.88 \pm 33.16$. Assuming $\theta_o = 0.442$ m^3 m^{-3}, the value of K is 1.04 mm day^{-1} for $\theta = 0.4$ m^3 m^{-3}. If this value of θ has an error of 2%, which is very small for field conditions, we would have θ ranging from 0.392 to 0.408 m^3 m^{-3}, and the corresponding values of K are: 0.43 and 2.55 mm day^{-1}, with a difference of almost 500%. This example shows in a simple manner the effect of the exponential character of the K(θ) relations. The standard deviations of K_o and β, shown above, reflect the problem of spatial variability. Added to this is the spatial variability of θ itself.

4.6 Changes in Soil Water Storage ΔS

Soil water storages S, defined by equation (6) are, in general, estimated either by: (i.) direct auger sampling; (ii.) tensiometry, using soil water characteristic curves; and (iii.) using neutron probes. The direct sampling is the most disadvantageous due to soil perforations left behind after each sampling event. Tensiometry embeds the problem of the establishment of soil water characteristic curves, and neutron probes have calibration problems.

Once θ *versus* z data at fixed times are available, S is estimated by numerical integration, the trapezoidal rule being an excellent approach, and in this case, equation (6) becomes:

$$S = \int_0^L \theta dz \cong \sum \theta \Delta z = \overline{\theta} L \quad \text{.....(8)}$$

The changes ΔS are simply the difference of S values obtained at different times.

ELECTROMAGNETIC WAVE ATTENUATION IN SOIL PHYSICS

K. Reichardt[1]; O.O.S. Bacchi[2]; J.C.M. Oliveira[2]; J.E. Pilotto[2]

1. INTRODUCTION

This text is a continuation of Bacchi and Reichardt (1993) and the simbols & definitions there used are also here used. Electromagnetic waves of high energy, like gamma-rays and X-rays, have the property of penetrating into relatively dense materials, and are therefore very useful for "inside" inspections. The attenuation of a beam of this radiation kind of is a function of the "density" of the material, and this fact opens the possibility to stutdy several materials, including the soil. We will here give more emphasis to the measurement of soil water contents and bulk densities, but also extend the technique to soil mechanical analysis.

2. GAMMA AND X RAY PROPERTIES

Gamma and X rays are electromagnetic waves which propagate in vacuum with the speed of light c, and have a characteristic wavelength λ (or frequency f) and, therefore, a characteristic energy E:

$$E = hf \; ; \; c = \lambda.f = \text{constant}$$

h being Plank's constant.

Radiation	wave length λ (μm)
gamma	$4x10^{-6}$-$1x10^{-4}$
X	$1x10^{-5}$-$1x10^{-2}$
Ultra violet	0.01-0.38
Visible light	0.38-0.78
Infrared	0,78-1.000

Gamma rays are originated from unstable nuclei, while X rays are the consequence of electron energy loss during target bombardmentor due to jumps between different energy levels (orbits). Therefore, gamma-ray beams are obtained from radiactive nuuclei and X-rays from "tubes" in which accelerated electrons loose energywhen interacting with targets, or electrons which are excited and when returning to their original levels, emitt radiation. Table 1 lists radioisotopes used as gamma-radiation sources. From these, the most commonly used are Americium, Cesium and Cobalt.

[1]Department of Physics & Meteorology – College of Agriculture (ESALQ) and Soil Physics Laboratory – Center for Nuclear Energy in Agriculture (CENA), University of São Paulo. Caixa Postal 96, 13400-970 Piracicaba (SP), Brazil.

[2]Soil Physics Laboratory – Center for Nuclear Energy in Agriculture (CENA), University of São Paulo. Caixa Postal 96, 13400-970 Piracicaba (SP), Brazil.

Table 1. Radioisotopes suitable for gamma attenuation experiments.

Radioisotopes	Half-life (years)	Main energy peaks (%)	(KeV)	
^{241}Am (Americium)	458	86	60	
^{109}Cd (Cadium)	1.24	100	88	
^{144}Ce (Cerium)	0.78	11	134	
^{134}Cs (Cesium)	2.50	23	570	
^{137}Cs (Cesium)	30	85	662	
^{60}Co (Cobalt)	5.3	100	1173	
^{192}Ir (Iridium)	0.2	29	296	
			20	308
			81	317
			49	468
^{22}Na (sodium)	2.6	100	511	
		100	1275	

When gamma radiation interacts with matter, mainly three processes occur, which are responsible for the attenuation of the beam. For low energy radiation the photo-electric process is very probable. By this process, the photon (or gamma ray) colides with an inner shell electron, is completely absorbed, and as a consequence the electron is ejected from the atom. For medium energy photons the Compton-effect is the most probable. Here a photon also colides with an electron, but there is only partial energy loss and the ray is deviated from its original trajetory. Through this process gamma and X radiation is scattered. Only for energies higher than 1.02 MeV, photons may interact with target nuclei and become transformed in an electron and a positron. This process is called pair-production.

Due to these and other less probable processes, a gamma-ray beam of a given intensity becomes attenuated when passing through matter. The attenuation process depends on the energy of the photons, on the nature and density of the target matter and on the length of the travel path of the radiation through this matter. For a mono-energetic radiation bean, Beer's law is valid:

$$I = I_o \exp(-k\rho x) \qquad (1)$$

where I_o is the incident beam intensity [number of photons per cm^2 per s, or counts per s (cps), or counts per minute (cpm)]; I the transmitted beam intensity; k the mass attenuation coefficient (cm^2/g); ρ the density of the absorbing material (g/cm^3); x the absorbtion length (cm). Figure 1 ilustrates the process.

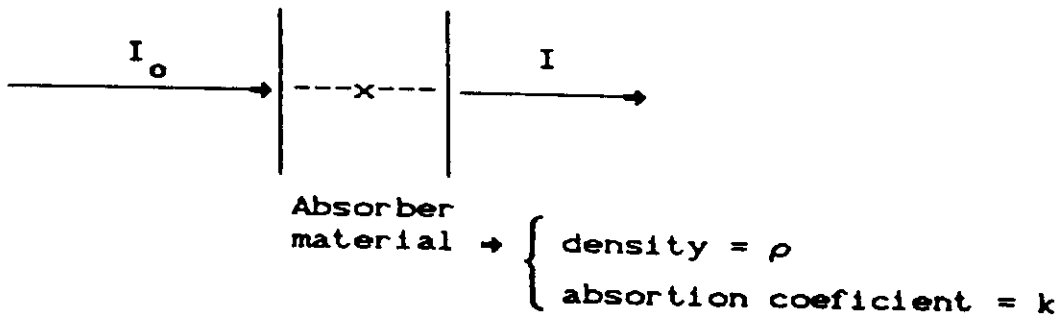

Figure 1. Schematic diagram of the attenuation process of a monoenergetic radiation beam by an homogeneons material

The absorption coefficient k is a function of the absorbing material and of the energy of the gamma or X rays. Knowing k and measuring I_o and I, the attenuation process can be used to measure ρ if x is known, or to measure x if ρ isknown, using equation (1). This is the principle of the process.

Very important details, which will not be treatet here, are i. source intensity; ii. beam colimation; iii. counting equipment; iv. peak definition, etc. Radiation safety has also to be mentioned. In general, to colimate radiation beams, gamma sources or X-ray tubes, are involved in lead (Pb) shields, calculated to protect the opperator. Radiation is only alowed to pass through a colimation whole, which defines the cross section of the beam (circular, rectangular, generally with less than 1 cm^2). At the beam, radiation levels are high and care showld be taken in order not to expose hands and other parts of the body to radiation. When manipulating samples within the beam path, the colimation whole should be closed with a lead shield.

3. ATTENUATION IN SOILS

Soils are not homogeneous and equation (1) must be extended for heterogenous materials. We will assume that the solid fraction of one given soil is homogeneous and so a moist soil sample of thickness x can be represented by:

$$x = x_s + x_w + x_a \qquad (2)$$

where $x_s + x_w + x_a$ are the equivalent thicknesses of solids, water and air, within x.

Since a soil sample generally comes in a container, and the radiation source is located at a "fair" distance from the radiation detector the total radiation absorbing distance X from source to detector will be:

$$X = x_{a1} + 2x_c + x_s + x_w + x_a + x_{a2} \qquad (3)$$

Figure 2 ilustrates schematially these distances. Considering the attenuation process as additive, equation (1) for the sistem described in Figure 2, is extended to:

$$I = I_o \exp\{-[k_a\rho_a(x_{a1} + x_a + x_{a2}) + 2k_c\rho_c x_c + k_s\rho_s x_s + k_w\rho_w x_w]\} \qquad (4)$$

where k_i, ρ_i and x_i correspond to material i.

If I_o is measured with the empty container, the constant attenuation of air and container is already taken care of, and recognizing that:

$$\rho_s x_s = d_b x \quad and \quad \rho_w x_w = \theta x$$

where: ρ_s = density of soil particles
d_b = soil bulk density
ρ_w = density of water
θ = soil water content

equatio (4) reduces to:

$$I = I_o \exp[-x(k_s d_b + k_w \theta)] \qquad (5)$$

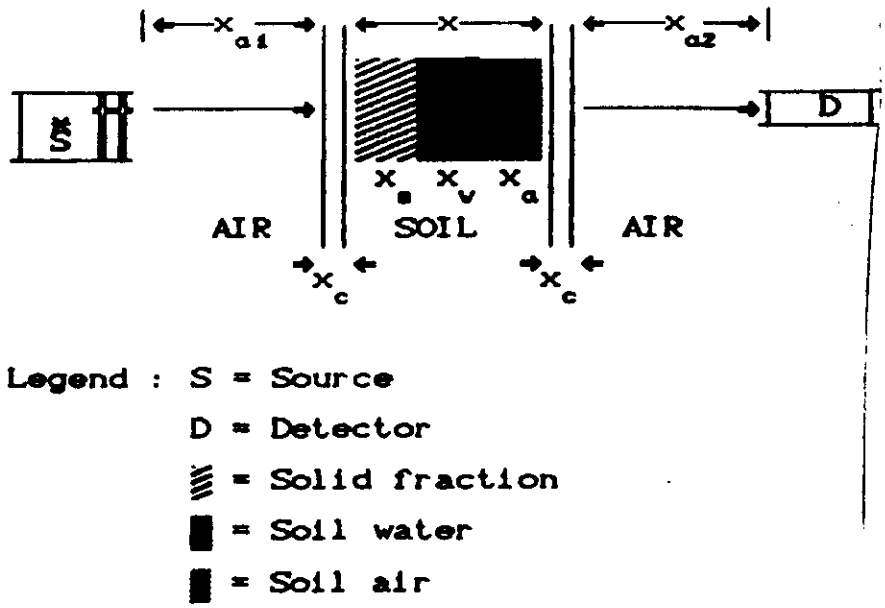

Figure 2. Schematic diagram of attenuation distances for a soil sample packed in a container.

Using carefully measured values of I_0, I, x, k_s and k_w, soil bulk density d_b and soil water content θ, can be estimated, at the position of the path of the radiation beam. Rearranging equation (5) we have:

$$d_b = \frac{1}{xk_s}\left[\ln\left(\frac{I_0}{I}\right) + xk_w\theta\right] \tag{6}$$

and

$$\theta = \frac{1}{xk_w}\left[\ln\left(\frac{I_0}{I}\right) + xk_s d_b\right] \tag{7}$$

The great difficulty in using equations (6) and (7) is that to measure d_b one needs to know θ and to measure θ one needs know d_b. For monoenergetic gamma or X-ray beams, the only possibilities are the measurement of d_b in dry soils ($\theta = 0$) and the measurement of θ in soil with d_b invariant in time and in θ, with previons measurement of d_b.

Since k_s and k_w are a function of the energy of the radiation, if a convenient choice of a double-energy (E_1 and E_2) radiation beam is made, which determine different values of k_s and k_w, soil bulk density d_b and soil water content θ can be measured simultaneonsly solving the set of equations:

$$For\ E_1:\ I_1 = I_{01} \exp\left[-x(k_{s1}db + k_{w1}\theta)\right] \tag{5a}$$

$$For\ E_2:\ I_2 = I_{02} \exp\left[-x(k_{s2}db + k_{w2}\theta)\right] \tag{5b}$$

The solution is:

$$d_b = \frac{\left[k_{w1}\ln\left(\frac{I_2}{I_{02}}\right) - k_{w2}\ln\left(\frac{I_1}{I_{01}}\right)\right]}{x(k_{s1}k_{w2} - k_{s2}k_{w1})} \quad (8)$$

$$\theta = \frac{-\left[k_{s1}\ln\left(\frac{I_2}{I_{02}}\right) - k_{s2}\ln\left(\frac{I_1}{I_{01}}\right)\right]}{x(k_{s1}k_{w2} - k_{s2}k_{w1})} \quad (9)$$

The use of equations (6), (7), (8) and (9) implies in the knowledge of the attenuation coefficients k_i. Ferraz and Mansel (1979) present values for several soils and for water, for several radiation energies. Some of them are reproduced in table 2. As can be seen from the k_i values of soils, for Americium and for Cesium, these two sources are a very good choice for a double energy beam. Since k_i values vary from soil to soil, they have to be determined for each soil. This is easily done through equation (1), using an artificially packed dry soil sample of known bulk density d_b.

Table 2. Soil and other absorber materials mass attenuation coefficients k_i for 60 (^{241}Am) and 662 (^{137}Cs) KeV gamma photons.

Material	Clay	Silt	Sand	k_i ($cm^2.g^{-1}$)	
	%			60 Kev	662 Kev
Dark red latosol	48	31	21	0.31647	0.07424
Yellow red latosol	17	10	73	0.27501	0.07834
Red yellow podsol	8	10	82	0.26411	0.07755
Alluvial soil	33	43	24	0.30440	0.07837
Regosol	16	9	75	0.25518	0.07724
Washed sand	-	-	100	0.25008	0.07666
Water (distilled)	-	-	-	0.20015	0.08535

Example 1: To measure the mass absorbtion coefficient of a soil for the gamma radiation of ^{137}Cs (622 KeV)), a dry soil sample was used, of thickness 5.7 cm and a bulk density of 1.473 g.cm^{-3}. The measured gamma intensities were I_o = 102525 cpm (container without soil) and I = 53575 cpm (container with homogeneously packet dry soil). In this case:

$$53575 = 102525 \exp(-k_s \times 1.473 \times 5.7)$$

and

$$k_s = 0.0773\ cm^2.g^{-1}$$

Example 2: Using the same container filled with distilled water, the attenuated gamma intensity changed to I = 63156 cpm. Therefore:

$$63156 = 102525 \exp(-k_w \times 1.000 \times 5.7)$$

and

$$k_{ww} = 0.085\ cm^2.g^{-1}$$

Example 3: A soil sample of thickness 6.62 cm is submitted to a double gamma ray beam and the following data was obtained:

Radiation 1:	Radiation 2:
$I_{01} = 253.428$ cpm	$I_{02} = 116.438$ cpm
$I_1 = 4.776$ cpm	$I_2 = 48.574$ cpm
$k_{s1} = 0.40139\ cm^2.g^{-1}$	$k_{s2} = 0.07881\ cm^2.g^{-1}$
$k_{w1} = 0.20015\ cm^2.g^{-1}$	$k_{w2} = 0.08535\ cm^2.g^{-1}$

Using equations (5a) and (5b) we have:

$$4.776 = 253.428 \exp[-6.62(0.40139 d_b + 0.200156)]$$

$$48.574 = 116.438 \exp[-6.62(0.07881 d_b + 0.085356)]$$

and solving this set of equations we obtain:

$$d_b = 1.340\ g.cm^{-3} \quad and \quad \theta = 0.310\ cm^3.cm^{-3}$$

4. EXPERIMENTAL ERRORS ASSOCIATED IN d_b AND θ MEASUREMENTS

4.1. Sample Thickness x

Sample tickness x is critical and has to be measured carefully, with minimal errors. In example 3 (above) if x would be 6.52 insted of 6.62 cm, i.e. with an error 1.5 of %, the values of d_b and θ would be 1.361 and 0.314, res,pectively.

Since the radiation attenuation process is exponential, the reduction of I_0 is very high, and directly related to the sample thickness x. In Example (3) we observe a reduction of I_0 of 98% for radiation 1 (low energy) and of 58% for radiation 2 (high energy). If x is increased excessively the values of I become too small, compromising counting statistics. Ferraz and Mansel (1979) show there is an optimum thickness x^*, which depends on the type of radiation and of the values of d_b and θ. Too thin samples or too large samples introduce great errors in the measurements. They show that x^* is given by:

$$x^* = \frac{2}{k_s d_b + k_w \beta} \qquad (10)$$

For example 3 we have:

$$\textit{Radiation 1:}\quad x_1^* = \frac{2}{0.40139\ x\ 1.34 + 0{,}20015\ x\ 0.31} = 3.3\ cm$$

$$\textit{Radiation 2:}\quad x_2^* = \frac{2}{0.07881\ x\ 1.34 + 0{,}08535\ x\ 0.31} = 15.1\ cm$$

Since x is more critical for the low energy, when using double beams, x has to be closer to x^* for the low energy. For the above example, $x = 6.62$ is a good choice. More details for the choice of x are found in Ferraz and Mansel (1979).

4.2. Errors in d_b and θ Measurements

Ferraz and Mansel (1979) show that the mininum resolvable changes σ of d_b and θ, when using a monoenergetic beam, are:

$$\sigma_{d_b} = \frac{1}{x k_d \sqrt{I_o}} \exp\left[\frac{x}{2}\left(k_e d_b + k_w \theta\right)\right] \qquad (11)$$

$$\sigma_\theta = \frac{1}{x k_w \sqrt{I_o}} \exp\left[\frac{x}{2}\left(k_e d_b + k_w \theta\right)\right] \qquad (12)$$

As can be seen, the mininum resolvable changes σ depend on all parameters and measurements of the attenuation process: I_o, x, k_e, k_w, d_b and θ. For example 3 analysing separately the case of each radiation, we have,

Radiation 1:

$$\sigma_{d_{b1}} = \frac{1}{6.62 x 0.40139 (253428)^{1/2}} \exp \left[\frac{6.62}{2}(0.40139 x 1.43 + 0.20015 x 0.31)\right]$$

$$\sigma_{\theta_1} = \frac{1}{6.62 x 0.20015 (253428)^{1/2}} \exp \left[\frac{6.62}{2}(0.40139 x 1.43 + 0.20015 x 0.31)\right]$$

and

$$\sigma_{d_{s1}} = 0{,}006\ g.cm^{-3} \quad ; \quad \sigma_{\theta_1} = 0{,}012\ cm^3.cm^{-3}$$

Radiation 2:

$$\sigma_{d_{s2}} = \frac{1}{6.62x0.07881(116438)^{1/2}} \exp$$

$$\left[\frac{6.62}{2}(0.07881x1.43 + 0.08535x0.31)\right]$$

$$\sigma_{\theta_2} = \frac{1}{6.62x0.08535(116438)^{1/2}} \exp$$

$$\left[\frac{6.62}{2}(0.07881x1.43 + 0.08535x0.31)\right]$$

and

$$\sigma_{d_{s2}} = 0{,}009\ g/cm^3 \quad ; \quad \sigma_{\theta_2} = 0{,}008\ cm^3/cm^3$$

indicating errors of about 0.5% for bulk density and 3.2% for water content measurements.

When using the double beam, a system of equations is solved and parameters of both radiations interfere in the measurements of d_s and θ. For this case:

$$\sigma_{d_s} = \frac{\left[\frac{(k_{w1})^2}{I_2} + \frac{(k_{w2})^2}{I_1}\right]^{1/2}}{x(k_{s1}k_{w2} - k_{s2}k_{w1})} \tag{13}$$

$$\sigma_{\theta} = \frac{\left[\frac{(k_{s1})^2}{I_2} + \frac{(k_{s2})^2}{I_1}\right]^{1/2}}{x(k_{s1}k_{w2} - k_{s2}k_{w1})} \tag{14}$$

For example 3, using the double beam, we have:

$$\sigma_{d_b} = \frac{\left(\frac{0.20015^2}{48574} + \frac{0.08535^2}{4776}\right)^{1/2}}{6.61(0.40139x0.08535 - 0.20015x0.07881)} = 0.012\ g/cm^3$$

$$\sigma_\theta = \frac{\left(\frac{0.40139^2}{48574} + \frac{0.07881^2}{4776}\right)^{1/2}}{6.61(0.40139x0.08535 - 0.20015x0.07881)} = 0.018\ cm^3.cm^{-3}$$

indicating errors of 0.8% and 5.8% for d_b and θ respectively. As can be seen, although the double gamma technique is an improvement, the measurements have greater errors as compared to the mono gamma technique.

5. FURTHER IMPROVEMENTS OF THE TECHNIQUE

One shortcomming of the gamma or X-ray attenuation technique is the measurement of x, which is critical for the estimation of d_b and θ, and difficult to be measured accurately. It is only easy to be measured for cases of soil samples packed in rectangular or cylindric acrilic containers, precisely manufactured. In other cases, like plants growing in commercial soil pots or even soil clods, it is very difficult to measure x, which varies for each measurement point.

Why not use a triple energy beam and leave x also as an unknown? This is not possible because x multiplies d_b and θ in equation (5) and the resulting simultaneous equations will not be independent.

So, as things stand today, x has to be meaured as precisely as possible for mono-and double beam attenuation measurement. One improvement has, however, been introduced through the computed tomography. This technique, first introduced into Soil Science by Crestana et al (1985) gives d_b and θ distributions in irregularly shaped soil samples, without the need of measuring x. In a tomograph the sample rotates around an axis and a very high number of attenuation measurements is made within the rotation plane, which envolve different beam paths, each having its x, d_b and θ. Solving all these unknowns through computation one obtains the d_b or θ distribution over the rotation plane, i.e., a cross section "picture" is obtained, indicating the d_b or θ distribution, with a resolution (pixel) that can go down to 1 mm^2. Vaz et al (1992) gives more details of the technique.

6. APPLICATIONS IN SOIL PHYSICS

6.1. Infiltration tests in homogeneous soils

The gamma-attenuation techniques is very suitable for laboratory studies that envolve water movement in soils. The main advantage of the methodology is its non-destructive character. As water moves thorough the soil, the changing water content can be monitored at different positions and times, with measurement times of less than 1 minute per point. Infiltration tests are examples for which gamma-attenuation has contributed singnificantly. These tests are normally performed on homogeneous soil columns, as shown in Figure (3). The colunns are packet carefully with dry soil and before submitting to water infiltration are tested for homogeneity through bulk-density distributions. This can be performed by gamma-attenuation and, when the colimation beam is of the order of mm, d_b can be measured mm by mm. Columns presenting undesired d_b descontinuities can be descarted and repacked.

During infiltration tests the position of the water wetting front x_f advances and it is important to know the θ distribution between $x = 0$ and $x = x_f$. Therefore, from time to time attenuation measurements are performed at points x, $0 < x < x_f$, since for $x > x_f$ we have only dry doil. This can be done in two ways. One is making quick θ measurements at several positions, starting close to x_f, because there θ changes rapidly, and then making measurements at increments Δx, approaching $x = 0$. In this case we obtain a x versus θ profile at a given time t^*, as shoun in figure 4.

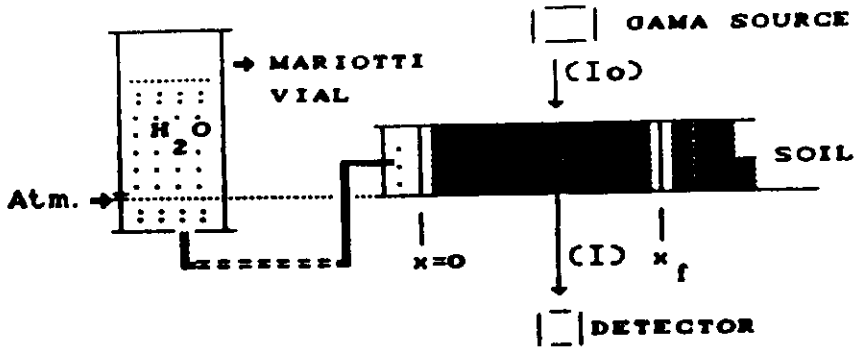

Figure 3. Schematic diagram of an infiltration test.

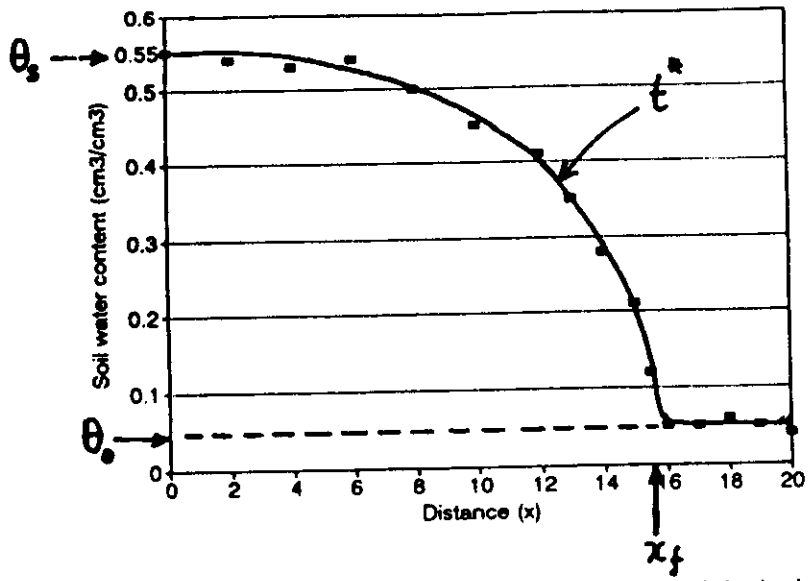

Figure 4. Soil water content at t^*; θ_s is the saturated water content and θ_o is the initial soil water content, in this case the water content of air-dry soil.

This procedure is only possible for soils with low infiltration rate, since the profile changes in time. If the wetting front position x_f does not change significantly in, let's say, 15 minutes, there is plenty of time to obtain the profile. Any way, allways starting at x_f and going backwords toward $x = 0$, where θ changes are slow. Even for soils of relatively fast infiltration rates this procedure is possible if the profile is measured for large times t^*, at which the infiltration rate has decreased significantly.

The other way, in cases of rapid changes in θ at measurement poitions, it is recomended to make several measurements at a fixed point x_i, then move to another point x_j and make another set of measurements, move to x_k and ..., and then return to x_i to make another set ... As a result one obtains θ versus t graphs, at choosen posions x (Figure 5). With this set of data it is possible to construct θ versus x profiles like Figure 4, for fixed times. In Figure 5, for example, we have θ values at positions x_i, x_j and x_k at exactly t_k.

The gamma-attenuation technique has been widely used in studies similar to the above. Just to mention some, the reader is reffered to Davidson et al (1963) and Reichardt et al (1972).

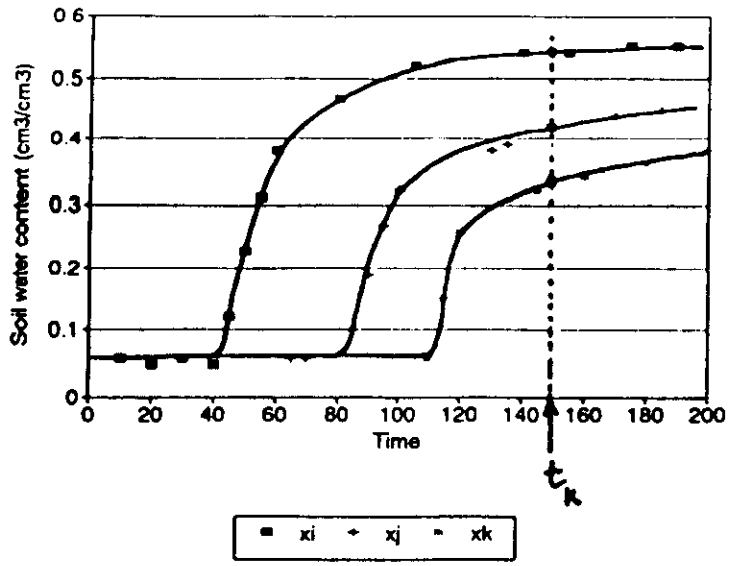

Figure 5. Soil water content as a function of time at three fixed positions.

6.2. Soil Mechanical analysis

The intensity of a gamma beam passing through a soil suspension at a given depth is related to the concentration of the suspension as it varies with time. From the changes in the attenuation of the beam intensity it is possible to calculate particle fractions. The attenuation equation for a gamma beam passing through the sedimentation system composed of an acrylic plastic container, soil particles, water and sodium hydroxide (shown in Figure 5) can be written as:

$$I = I_0 e^{-(k_w x_w + k_s d_p x_p)} \qquad (15)$$

where I_0 is the attenuated radiation beam (cps) from the system without the soil, I the attenuated radiation beam (cps) from the system with soil under sedimentation, k_w and k_s ($cm^2 g^{-1}$) the mass attenuation coeficients for water and soil, respectively; x_p (cm) the absortion thickness due to soil particles; and d_p ($g.cm^{-3}$) the particle density. Equation (15) neglects the absortion thickness of sodium hidroxide, assumes that the density of the solution is 1 $g.cm^{-3}$ and assumes that all particles have the same density.

Relating the suspension concentration C ($g.l^{-1}$) to the particle density and to the container internal thicknees $\underline{X}$ (cm), we have:

$$x_p = \frac{C \cdot X}{d_p} 10^{-3} \qquad (16)$$

Substituting (16) into (15) we obtain:

$$C = \frac{\ln(I_o/I)}{X\,(k_s - k_w d_p)} \qquad (17)$$

Equation (15) is obtained as follows:

$d_p = m_p/v_p$ (a)

$C = m_p/v$ (b)

$d_p . v_p = C . v$. (c)

$d_p/C = v/v_p$ (d)

$$\frac{d_p}{C} = \frac{A \cdot X}{A \cdot x_p} \quad (e) \qquad \frac{d_p}{C} = \frac{X}{x_p} \qquad (15)$$

From the measurement of I as a function of the sedimentation time at a chosen depth h (equivalent to the pipette depth) the suspension concentration is obtained by equation (17). Knowing the initial suspension concentration the percentage of each particle size fraction can be calculated. Since the measurements of I are performed in definite time intervals (Δ_t = 3 seconds), it is difficult to measure the initial concentration (corresponding to the start of the sedimentation process, t = 0) through beam attenuation. Therefore, the initial concentration is calculated from soil mass and solution volume.

A radiactive source ^{241}Am of 300 mCi is used to produce the gamma-ray beam, using the energy peak of 59.6 Kev. The detection system is composed of a NaI(Tl) crystal scintilator, photomultiplier cell, power supply, amplifier, monochannel analyser and counter timer. To improve the sensibility of the method, the beam colimator can be a horizontal rectangular slot (1 mm x 15 mm) instead of the traditionaly used cirular colimator. More details can be found in Vaz et al (1992).

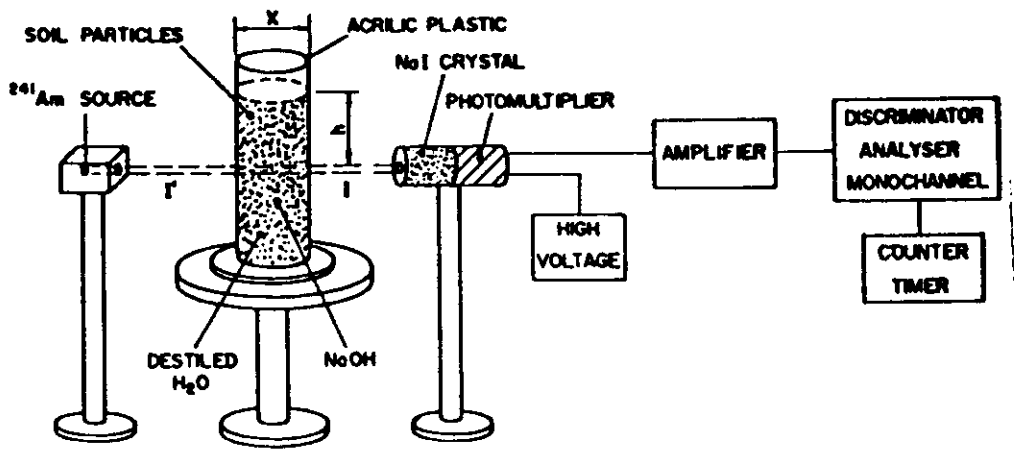

Figure 6. Scheme of the gamma ray attenuation system.

7. REFERENCES

BACCHI, O.O.S. and REICHARDT, K. 1993. Neutron probes and their use in gronomy. CENA, P.O. Box 96, 13418-900. Piracicaba, S.P., Brazil. 54p.

CRESTANA, S.; MASCARENHAS, S. and PAZZI-MUCELLI, R.S. 1985. Static and dynamic three dimensional studies of water in soil using tomographic scanning. Soil Science, Baltimore, 140(5): 326-332.

DAVIDSON, J.M.; NIELSEN, D.R. and BIGGAR, J.W. 1963. The measurement and description of water flow through Columbia Silt Loam and Hesperia Sandy Loam. Hilgardia, Davis, 34: 601-617.

FERRAZ, E.S.B. and MANSELL, R.S. 1979. Determining Water Content an Bulk Density of Soil by Gamma Ray. Attenuation Methods. Bull 807 (Tech.) Univ. of Florida, Gainsville, USA, 43p.

REICHARDT, K.; NIELSEN, D.R. and BIGGAR, J.W. 1972. Scaling of horizontal infiltration into homogeneous soils. Soil Sci. Soc. Am. Proc., Madison, 36: 241-245.

VAZ, C.M.P.; CRESTANA, S.; MASCARENHAS, S.; CRUVINEL, P.E.; REICHARDT, K. and STOLF, R. 1989. Using a computed tomography miniscaner for studying tillage induced soil compaction. Soil Technology, Cremlingen, 2: 313-321.

VAZ, C.M.P.; MARTINS, J.C.O.; REICHARDT, K.; CRESTANA S. and CRUVINEL, P.E. 1992. Soil mechanical analysis through gamma-ray attenuation. Soil Technology, Cremlingen, 5(4): 314-325.

NEUTRON PROBES AND THEIR USE IN AGRONOMY

O.O.S. Bacchi[1]; K. Reichardt[2]

1. INTRODUCTION

Neutron probes were developed to measure soil water contents in agricultural field soils. Soil water content, although being a very simple soil physics concept,is very difficult to be evaluated in the field. Estimatives of soil water content obtained through many methods often deviate considerably from the "true" value, which, anyway, is never known. The main problem lies in sampling procedures. Once a soil sample is taken from the field and brought to the laboratory, its soil water content can be estimated with a high degree of precision and accuracy. It is, however, never known if collected sample realy represents the soil at the desired depth, mainly due to soil variability and sampling procedures.

Soil water content can be estimated on a weight or a volume basis. In this work we will use the following simbols and definitions:

a) soil water content by weight u (g H_2O/g dry soil)

$$u = \frac{\textit{mass of water}}{\textit{mass of dry soil}} = \frac{m_w - m_d}{m_d} \qquad (1)$$

where: m_w = mass of wet soil
m_d = mass of dry soil

b) soil water content by volume θ (cm^3 H_2O/cm^3 of bulk soil)

$$\theta = \frac{\textit{volume of water}}{\textit{bulk volume of soil}} = \frac{m_w - m_d}{V} \qquad (2)$$

where V is the volume of the soil sample. In this definition it is assumed that the density of water is 1 g/cm^3 and, therefore, (m_w - m_d) is equal to the volume of water.

It can be shown that

$$\theta = u.d_b \qquad (3)$$

where d_b is the bulk density of a dry soil (g dry soil/cm^3 of bulk soil), defined by:

---

[1]Soil Physics Laboratory – Center for Nuclear Energy in Agriculture (CENA), University of São Paulo, Caixa Postal 96, 13400-970 Piracicaba (SP), Brazil.

[2]Department of Physics & Meteorology - College of Agriculture (ESALQ) and Soil Physics Laboratory - Center for Nuclear Energy in Agriculture (CENA), University of São Paulo, Caixa Postal 96, 13400-970 Piracicaba (SP), Brazil.

$$d_b = \frac{m_d}{V} \qquad (4)$$

Example: In a soil profile, a soil sample was collected at the depth of 20 cm, with a volumetric cylinder of 200 cm^3 and 105.3 g. After handling the sample in the laboratory, eliminating all excess of soil from the out side of the cylinder and being sure that the soil was ocupying the volume V of the cylinder, the sample was weighed and the result was 395.6 g. The sample was then introduced into a ventilated oven at 105°C, until constant weight, and the final mass was 335.7 g. In this case:

$$u = \frac{395.6 - 335.7}{335.7 - 105.3} = 0.260 \frac{g}{g} = 26.0\% \ \textit{weight}$$

$$\theta = \frac{395.6 - 335.7}{200} = 0.300 \frac{cm^3}{cm^3} = 30.0\% \ \textit{volume}$$

$$d_b = \frac{335.7 - 105.3}{200} = 1.152 \ g/cm^3$$

and accordind to equation (4): 0.300 = 1.152 x 0.260.

There are several methods for the determination of soil water contents and bulk densities. They differ mainly in the form of sampling, but equations 1 to 4 are always applicable when information is available. The greatest difficulty lies in the measurement of V. Sampling soil with a simple auger destroys the structure of the soil and the information about V is lost. In this text we will not discuss all these "classical" methods of soil water measurment. The reader is refered to any basic soil physics text, or specifically to "Methods os Soil Analysis", part I, American Society of Agronomy, Monograph n° 9, 1986.

We will, however, discuss some aspects of the classical methods in order to compare them with the neutron probe method, which will be treated in detail. One great disadvantage of the classical methods is their destructive feature. We have to sample the soil at each measuring event and intefere severely in the soil profile. Even sampling with a simple auger, after several samplings the field or plot will be very disturbed. Another problem is soil variability. At each sampling event, even collecting soil at the "same" depth, another location is sampled. A third problem, which might be minor, is the time spent for one measurement, which is almost never below 24 hours.

With neutron probes, which we will discuss in detail in the folowing pages, we disturbe less the soil profile. Only once an access tube has to be introduced into the soil to the desired depth and, thereafter, measurements are taken at any depth and time in a matter of minutes. Of course, there are also disadvantages in the use of neutron probes. At the end of this text we will spend some time discussing advantages and disadvantafes of their use.

2. INSTRUMENT DESCRIPTION AND WORKING PRINCIPLE

A neutron probe consists essentially of two parts: (a) shield with probe, and (b) electronic counting system. In some models these parts are separable and in others not.

(a) Shield with probe

The probe is a sealed metalic cylinder of diameter 3 to 5 cm and length 20 to 30 cm. It contains a radioactive source which emitts fast neutrons, a slow neutron detector and a pre-amplifier. The signal of the pre-amplifier goes through a 5 to 20 m long cable to the electronic counting system.

The geometry of the probe, type and activity of the neutron source, type of detector and pre-amplifier, vary considerably from manufacturer to manufacturer. Neutron sources are the mixture of an alfa particle emitter (like Americium, Radium) and a fine powder of Berilium. Alfa particles bombard Berilium nuclei and the folowing reaction takes place:

$$^{2}_{4}\alpha + ^{9}_{4}Be \rightarrow ^{1}_{0}n + ^{12}_{6}C + energy$$

The neutrons $^{1}_{0}n$, which are a product of the reaction, are called fast neutrons, having energies of the order of 2 MeV (1 eV = 1,6 x 10^{-19} j).

The strength of the sources are generaly given by the activity of the alfa emitter, in milicuries (mCi). Most of the sources have an activity in the range of 5 to 50 mCi. Since most alfa emitters also emitt some gamma radiation, the sources generally emitt alfa particles, gamma radiation and fast neutrons. Therefore, **radiation protection in an important issue**. The shield, which is the case for the probe, has to be designed in order to protect the user from the radiation. Manufactured probes that are sold comertially have a shield that exposes the user only to permissible radiation levels, when in the shield. When the probe is not in the protection shield, the user is exposed to gamma radiation and neutrons. This should be terminantely avoided. The design of the probes is done in such a way that when the probe leaves the shield it goes immediately into the soil, avoiding any excessive radiation exposure.

Shilding of gamma radiation is most efficiently made by lead and of fast neutrons by parafin, poliethilene or any other material with high H content. Neutron probe shields have, therefore, some metalic shield and some high Hydrogen content material.

During measurements, the probe is lowered to the desired depth in the soil, inside of an aluminum access tube. Aluminum is "transparent" to fast neutrons and so they are scattered into the soil, most of them not going further than 30 to 50 cm away from the source. This interaction with the soil (and soil water) is used to estimate soil water content, as will be seen later.

Next to te source is a slow neutron detector. This detector does not count fast neutrons, it detects only slow neutrons which are a result of the interaction of the fast neutrons with the soil. There are several slow neutron detectors available, e.g. Boron tri-fluoride detectors, Helium-3 detectors, and scintillation detectors. Each manufacturer makes its choice because all have advantages and disadvantages.

The pulses comming from the detector are first preamplified, which also occurs in the probe. Only these, slightly amplified pulses, are sent to the electronic counting system, through the cable which connects parts (a) and (b) of the neutron probe.

(b) Electronic counting system

The electronic counting system varies a lot from type to type of probe. In simple words, it constitutes of an amplifier, a high voltage source, a counter, a timer, rechargeable bateries, a microprocessor, etc. Since counting time is important for statictics, most probes have several options, e.g. 0.5, 1 and 4 min counting times. The microprocessor processes data and gives results in counts per minute (cpm) or counts per second (cps). Each count corresponds to one impulse originated from one slow neutron that reached the detector.

Recent neutron probes have a microprocessor to which one can feed the calibration equation for several soils, and the results are given directly in soil water content (%, g/g, cm^3/cm^3) or even in terms of a water storage in a given soil layer (mm/10 cm, inches/foot).

Each manufacturer gives details of the operation of their probe and, therefore, we will not discuss this matter here. Figure 1 is a shematic diagram of a depth neutron probe, in the field, in a measurement position at depth L. Figure 2 is a schematic diagram of a surface neutron probe, also in measurement position. These probes are made only for surface (0-15 cm depth) measurements and do not need access tubes. They are placed, between rows, on the soil surface.

The working principle of neutron probes is very simple and straightforward. The neutron source emitts fast neutrons (of the order of 2 MeV) which interact with the matter which sourounds the probe. Since neutrons have no charge, electric fields do not counteract their movement. Three processes occur during this interaction: neutron absorption by nuclei, neutron scattering through collisions, and neutron desintegration.

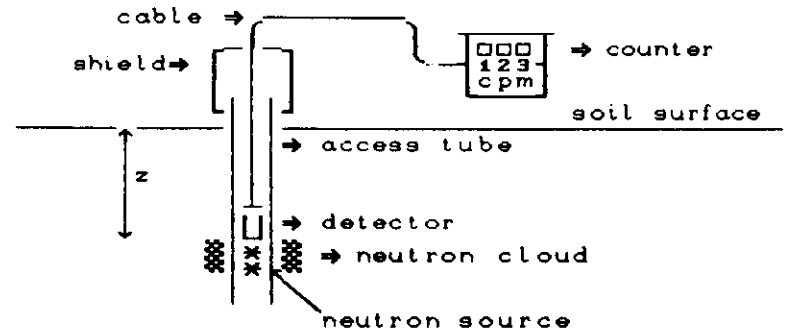

Figure 1. Depth neutron proble diagram at working position.

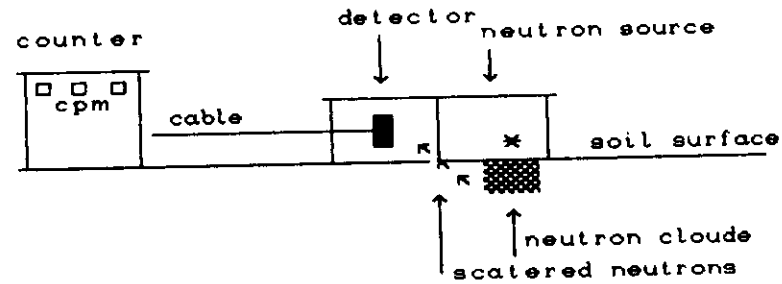

Figure 2. Surface neutron proble diagram at working position.

Neutron absortion by nuclei depends very much on the neutron energy and the type of target nucleus. The "probability" of this process is measured through the cross section of the reaction, which in general, for most of the elements present in soils, is very low. If the reaction occurs, one neutron is absorbed by a nuclews ${}^{Z}_{A}x$ according to:

$$ {}^{1}_{0}n + {}^{Z}_{A}X \rightarrow {}^{Z}_{A+1}X $$

where the new nucleus ${}^{Z}_{A+1}X$ is, in some cases, unstable and desintegrates emitting radiation. This is the same principle of neutron activation. The process, however, occurs only with a few nuclei present in the soil, e.g., Ag, Au, In, Fe, Al, Mn, etc, most of them having a very low concentration is soils. Also the neutron flux emitted by the source has generally a very low intensity so that the probability of a neutron capture is extremely low. In many cases ${}_{A+1}{}^{Z}X$ is stable (e.g., ${}^{12}C + n \rightarrow 13C$; ${}^{14}N + n \rightarrow {}^{15}N$) and in the cases it is radioactive (e.g., ${}^{23}Al + n \rightarrow {}^{24}Al$, half life of 2.3 min) its half-life is also generally very short. Due to these facts there is virtually no activaton of soil material when a neutron probe is placed into the soil. Also the Aluminum access tubes, which might become slightly active during one measurement, decais in a few minutes.

Neutron senttering by collisions (elastic or mon-elastic) is the most important process, on which the working principle of the neutron probe is based. Through collisions fast neutrons (high energy, about 2 MeV) loose energy (moderation) and might become slow or thermal neutrons (low energy, about 0.025 eV). If collisions are elastic, the heavier the target nucleus, the less energy is lost by the neutron. Table I illustrates this fact.

It can be seen that ${}^{1}H$ is the most efficient target atom for reducing neutron energy. It is said that Hydrogen is a good neutron moderator. Since Hydrogen is a constituint of water, water is also a good neutron moderator. So, in a given soil, the wetter it is, the more slow neutrons will be present in the presence of a fast neutron source. Other soil materials also have Hydrogen as a constituint but, in this case, its Hydrogen content is constant, and is taken into account during calibration. The only exception is organic matter.

Neutrons when free are unstable, they desintegrate with a half-life of 11 minutes. So, if a neutron is not captured it will, after some time, desintegrate according to:

$$ {}^{1}_{0}n \rightarrow {}^{1}_{1}p + \beta^{-} + \nu + 780\ KeV $$

Table 1. Number of elastic collisions necessary to reduce the energy of a neutron from 2 MeV to 0.025 eV.

Target Isotope	Number of Collisions
1_H	18
2_H	25
4_{He}	43
7_{Li}	68
12_C	115
16_O	152
238_U	2172

Due to these processes, after few fractions of a second, a stable "cloud" of slow neutrons is developed in the soil around the source, having a spherical shape, with a variable diameter of 15 to 40 cm. The number of slow neutrons per unit volume at each point of the cloud remains constant and is proportional to the water content of the soil within the cloud. Since the slow neutron detector is placed inside the cloud volume, the count rate (cpm or cps) is proportional to the soil water content θ of the same volume. The instrument is then calibrated with samples of known θ. More details about neutron moisture meter theory can be found in Greacen (1981) and IAEA (1970).

3. SAFETY AND MANTAINANCE

As already stated, neutron probes available in the marked are tested for radiation exposure and the opperator is exposed to radiation levels below the international permissible dosis. Attention has, however, to be given to:

a) Neutron probes, like any other instrument with radioactive material, should not be opperated by people with less than 18 years of age or not well instructed people.

b) During use opperator has to use a dosimeter for neutrons and gamma radiation.

c) Special attention to radiation exposure should be given when the probe is not in its shield. This should be avoided to a minimum and, when necessary, a radiation protection expert should be around.

d) Repair of problems in the probe (e.g., preamplifier, changing detector, fixing cable connection) should only be done by authorized people.

e) Probes should be stored in special dry places, designed for radioactive material storage, far from the circulation of other personnel.

f) For mantainance, each manufacturer gives details for their probes, but it is very important to mantain them in continuous use. Charging of batteries is very important. Therefore, even in periods when no experimental work is being carried out probes should be serviced once a week by an authorized technician, making at least a few standard counts.

4. ACCESS TUBES AND THEIR INSTALLATION

Size and type of access tubes depend on the diameter of the probe in use, cost and availability of tubing. Unfortunately diameters of probes have note been standardized internationally by manufacturesrs so that practically each probe has his own diameter and requeires specific tubing.

The best material is aluminum since it is very transparent to neutrons. Only in a few soils aluminum can corrode and be a problem for long term experiments. Other materials can also be used, e.g. steel, iron, brass, and also polyethilene and other plastics. It has only to be recognized that these different materials have

different behaviour with respect to neutron interaction and count rates will be altered. Once one kind of tubing is chosen, calibration and all experimental work have to be done with the same material.

It is know that steel and brass tubings affect slightly the sensitivity of probes due to the greater absorbtion of neutrons by iron and copper. Polyethilene and other plastic materials contain significant amounts of Hydrogen and, therefore, give a higher count rate.

Tube size is normally specified by each manufacturer through inside and outside diameters. One should keep the closest possible to these specifications, mainly to the inside diameter. Probe shoud not enter tightly into tubing and a great air-gap between probe and tube wall affects sensitivity.

Tube length depends on measurement depths which depends on the objectives of the experiment. Access tube should always be 10 to 20 cm longer than the greatest measurement depth because the "active center" of the probe is never at its end. Tubes should also extend 20 to 40 cm above soil surface, in order to avoid entrance of soil material and to facilitate the positioning of the shield case on top of the tube. Top end of the tube should be covered with rubber stoper or an inverted Aluminum beer can, to avoid water and dirt entrance. The botton of the aceess tube has also to be sealed (with rubber stoper or other material) if water table level is high. For very deep and aerated soil profiles this is not necessary.

There are several methods of installation of access tubes (Greace, 1981) but essentially they all consist in drilling an auger hole into which the access tube is driven down to the desired depth. The main point in this procedure is to avoid an air-gap between the soil and the tube. This might be achieved by using an auger with a slithtly smaller diameter than the outside diameter of the acces tube. In this case, the tube is introduced with difficulty into the soil and some soil might enter inside the tube. With a second auger, with a diameter slightly smaller than the inside diameter of the tube, the soil that entered inside the tube is removed. Some people prefere to introduce the access tube with impacts into the soil, in steps of about 20 cm and then eliminate the soil inside the tube with an appropriate auger. In this case, there is very good contact between soil and access tube. The inside of the tube has, however, to be cleaned very well.

In special cases, however, many problems might occur. As an example we refer to stony soils, heavy swelling soils and extremely layered soils. In each case, the researcher has to use his own experience and do his best. It should only be remenbered that the installation of an access tube is done only once for a given experiment and, therefore, it has to be done with much care, even if it takes a few hours. A badly installed access tube will compromise all measurements mad in future. It should also be remenbered that one of the great advantages of the neutron moderation method is the fact that tha only disturbance made on the soil is during access tube installation and that, thereafter, quick measurements can be made over long periods, always "sampling" the same "point" in the field.

Reapeting, time should therefore be spent to install in the best possible way each access tube. More details about access tube installation can also be found in IAEA (1976).

5. CALIBRATION

The calibration of a neutron probe consists in finding a relation between probe output: cpm (counts per minute) and soil water content θ (cm^3 of water per cm^3 of bulk soil). To do this, samples of a given soil having a wide range in moisture are used to measure cpm with the probe and θ in the classical way. It is a simple procedure in theory but it might be difficult and tedious depending on the choosen experimental design and of the properties of the soil profile. First we will disucss an easy case of the construction of the calibration curve for one depth of a homogeneous soil, and then extend it to more difficult situations.

Sampling is the main problem in calibration. In theory, the same sample should be "exposed" to the neutron probe to obtais cpm, and to the classical soil moisture method to obtain θ. This is very difficult in practice, mainly because the neutron method "sees" a great volume which is not well defined (assumed to be a sphere of 20 to 30 cm diameter) and the classical soil moisture methods use small samples (20 to 50 times smaller). This problem is minimized by taking several soil samples for θ determination around the access tube in which cpm was obtained. In any case, we are never sure that both methods sampled the same total volume of soil. This becomes worse in heterogeneous soils, like layered or stony soils.

Another problem is finding the same soil in a wide soil moisture content range. By wetting (irrigation or rainfall) and drying (evaporation of drainage) a good range can be obtained, but always over a long period ot time and wide range in space, and with tedious operations. Since the neutron probe "explores" a large sample, during wetting and during drying, we never know if the whole sphere of influence was submitted to the same intensity of drying or wetting.

Assuing we did our best and we have a good collection of pairs of cpm and θ data we can start constructing our calibration curve. First, in order to avoid electronic drifts, temperature and other effects on the electronics of the neutron probe, we do not use cpm obtained in soil directly, but use the count ratio CR defined as:

$$CR = \frac{cpm\ in\ soil}{cpm\ in\ standardmaterial} = \frac{N}{N_s} \qquad (5)$$

Every time the neutron probe is used, it is cheched for stability making a counting in a standard material which in most cases is taken with the probe inside its protection shield, sitting on the probe transportation case to mantain a standard condition. Others recommend a standard count in water. In this case a sealed access tube is placed in the center of a large water conainer. The standard count C_s (total number of counts taken over a time t_s) gives us a standard count rate $N_s = C_s/t_s$ which should be constant over long periods of time, oscilating only within the statistcal deviations, normally taken as $\pm \sqrt{C_s}$ (Poisson's distribution). Each manufacturer gives details for these procedures for their probes.

Table 2 shows field data obtained for the calibration of a probe for the 20 cm depth.

Table 2. Calibration data for probe SOLO 25 (made in France) with a 40 mCi Am/Be source. Soil: Terra Roxa Estruturada (Alfisol) of Piracicaba, SP, Brazil. Depth: 20 cm below soil surface.

nº of pairs n	θ ($cm^3.cm^{-3}$)	Count rate N (cpm)	Count Ratio CR*
1	0.424	79.650	0.507
2	0.413	75.541	0.481
3	0.393	76.169	0.485
4	0.387	71.143	0.453
5	0.378	67.846	0.432
6	0.375	69.259	0.441
7	0.306	59.208	0.377
8	0.287	57.637	0.367
9	0.291	62.035	0.395
10	0.283	58.109	0.370

*Count in water N_s = 157.050 cpm taken as standard.

Figure 3 shows the linear graph of θ versus CR. The solid line follows the equation θ = -0,0954 + 1.0424CR obtained through classical linear regression, using θ as the dependent variable y and CR as the independent variable x. The linear regresion coefficient was R = 0.9644.

As will be seen in next the chapter, the variances of the intersept and of the slope, and their covariance will contribute to a calibration error. This is one of the main errors in the use of neutron probes and, therefore, has to be minimized. In general, the closer to 1.0000 the value of R, the lower are these variances. This can be achieved by increasing the number of calibration points n, but they have to be "good points", that is, they should follow a straigh line behaviour. The best way is increasing n with points that widen the water content range, taking very wet (close to or at saturation) and very dry points.

The intersept a of a calibration curve varies from soil to soil and from probe to probe. It has not to be zero or close to zero, since it is an extrapolated value, out of the calibration range. No strong theoretical meaning should be given to a, but anyway, is related to the residual H content of the soil.

The slope b also varies from soil to soil and from probe to probe. It represetns the sensitivity of the probe, being the derivative of the calibration line y = a + bx, that is, b = dy/dx. It is therefore the change in water content (dy = dΘ) per unit change in count ratio (dx = dCR). The lower its value, the more sensitive is the probe. It means that for small changes in water content we have great changes in count ratio, which is the variable we measure.

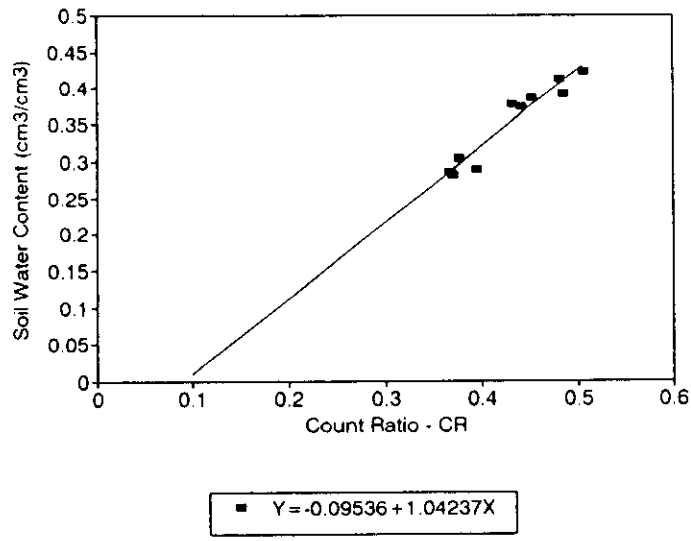

Figure 3. Calibration equation obtained with Table 2 data.

Because of the processes of neutron interaction in the soil, geometry of the probe, type of neutron detector, electronics etc, each soil has a specific calibration relation for a given neutron probe. Soil characteristics also affect the calibration relation, mainly the soil chemical composition and soil bulk density. Therefore, for a specific soil, calibration curves are related to different soil bulk densities d_b (figure 4). In general, the calibration lines for different bulk densities of the same soil are paralel, having the same slope b. For very layered soils, with layers of different composition, like some alluvial soils, the slopes for each layer might be different.

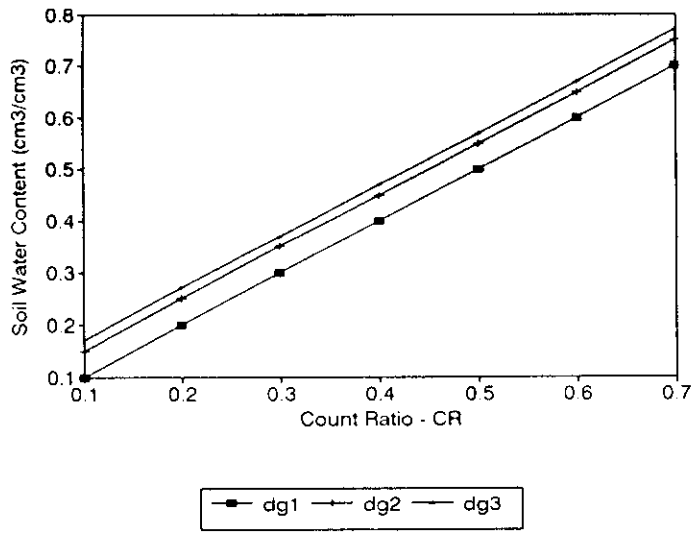

Figure 4. Schematic examples of calibration equations for different soil bulk densities.

Stony or gravely soils are a special problem. To begin with, access tube installation is difficult. The definition of Θ is also difficult, some authors use as bulk volume the total sample volume, including gravel, others exclude the volume occupied by gravel since it is a "dead" volume for water.

Every case is a different case and the neutron probe user will have to find out by himself details of obtaining the calibration curves. The necessity of different calibration curves for slightly different soils or for slightly different bulk densities will depend on the objectives of each experiment. The accuracy needed for the determination of Θ will the most important criterium for judgement.

In a very broad sense we can divide all calibration methodologies in three groups: laboratory, field and theoritical calibration.

Laboratory calibration envolves the use of packed soil samples with descrete levels of soil water content Θand soil bulk density d_b. For this, great amounsts of soil are packed into drums of 80 to 120 cm diameter and 80 to 120 cm height. Packing should be done carefuly in order to obtain a homogeneous sample in Θ and d_b.This is a very difficult task. The access tube is placed in the center of the drum.

Many neutron probe manufacturers have a collection of these sealed drums in order to calibrate each new probe. This data is given to the user and, normally, it is called factory calibration curve. Its use is very limited since it is done for one give soil. However it gives useful information to the user, when comparing this calibration relation to his own for a given soil. Commonly the slope b of these calibration curves is very similar. Because of this fact, many times one can use the factory calibration curve when the interest is only measuring soil water content changes ΔΘ, and not absolute values of Θ.

Field calibration envolves the installation of access tubes directly in the field and, at a certain soil water content situations, measurements of cpm are made with the probe and immediately after this soil samples are collected, at the same depths, around the access tube, to measure Θ by any classical method. This procedure is repeated to obtain the desired number of replicates, and repeated with the soil at different moisture conditions. Under field conditions it is difficult to find the soil in a wide range of soil moisture. To obtain very wet situations irrigation is the best way. Dry points are more difficult to obtain; it might take several weeks for the soil to become dry and, if it rains, one has to wait for another dry spel. The great problem lies in the fact that soils do not dry at a same rate at every depth and, as soill dries out it becomes heterogeneous with respect to moisture. This introduces an error in the calibration.

Theoretical models have also been developed in order to establish calibration relations, based on neutron diffusion theory. One of the most accpted models (Couchat et al., 1975) is based on the measurement of neutron absorbtion and diffusion cross sections in a graphite pile. Soil samples have to be sent to a specialized laboratory that has a graphite pile and that will establish a linear calibration equation as a funciton of θ and d_b.

Another great problem is establishing a calibration relation for the top surface layers. Many people recommend not to use the depth neutron probe for measurements close to soil surface, and use any other classical method. There are surface neutron probes, as shown in figure 2, which are specially designed for surface measurements.

Another approach is to obtain separate calibrations for shalow depths, which would take into account the escape of neutrons to the atmosphere. Some authors suggest to use neutron deflector/absorbers, which are parafin or poliethylene blocs, in the form of discs with a central whole, which are placed through the access tube on top of soil surface. Calibration is performed with the reflector. The use of these deflectors in routine measurements has, however, showed to be impractical in many situations. One recent and important contribution to the use of deflectors was given by Falleiros et al (1993).

6. "SPHERE OF INFLUENCE"

The slow neutron cloud which is formed immediatly after the probe is placed at a desired depth defines a sphere which is the volume of soil that the probe "sees". This sphere is called "**sphere of influence**" or "**sphere of importance**" of the probe. Unfortunately this sphere is not constant, not even for the same soil using a given probe. Theoretical studies (IAEA, 1970) show that its diameter is a function of the Hydrogen content (soil water content) of the medium. It is minimum in high Hydrogen content materials, like pure water, where it can take value of the order of 10 to 15 cm. In very dry soils, in which Hydrogen content is very low, the diameter of the "sphere of influence" can go up to 80 cm or more. Olgaard's (1969) theoretical model suggests that for values of $\Theta = 0.1\ cm^3/cm^3$ (which are extremely low for agronomic purposes) the diameter of the sphere is not greater than 90 cm.

This fact indicates a great sampling problem for every measurement made and also for calibraton. It means that for each soil water content Θ, the probe "sees" a different volume of soil. This is a problem we have to live with, and be careful, mainly when working at shallow depths in dry soils. It is therefore recommended to know the diameter of the "sphere of influence" as a function of Θ, and then, place the probe at the correct depth not to loose neutrons to the atmosphere.

To measure the diameter of the sphere of influence, the medium has to be homogeneous, and so it is best done with soil packed in drums. If a field soil is fainly homogeneous (also in Θ) the measurement can also be done in the field. The experimental procedure is very simple. The probe is lowered to a depth much greater than the radius of influeence R. Since R is not known, and it should not be greater than 45 to 50 cm, we lower

the probe down to 100 cm. Count rates are taken in very short depth intervals (if possible cm to cm, if not each 5 cm) bringing the probe up to soil surface. While the probe is at great depths, the sphere of influence is completely in the homogeneous medium, and count rates should be fairly constant, fluctuating only within the statistical permissible deviations ($\pm \sqrt{N}$, Poissons distribution). As the active center of the probe approaches soil surface, some neutrons start to escape to the atmosphere and the count rate starts to decrease. The decrease is first slow but soon goes exponentially close to zero, when most of the sphere is in the air. Due to this escape of neutrons the operator should take care of his protection, standing as far as possible from the probe. From the graph of the count rate as a function of depth it is possible to estimate the radius of the sphere of importance. At the depth where the count rate starts to decrease, the sphere starts to come out of the soil. This depth is its radius. Figure 5 and Table 3 ilustrate the procedure.

The recent work carried out by Falleiros et al (1993) extends the above methodology for heterogeneous soils or soils with heterogeneous water contents. In these cases, count rates are not constant with depth, even at great depths. making one set of measurements with a neutron deflector and another set without deflector, the radius of influence can easily be found.

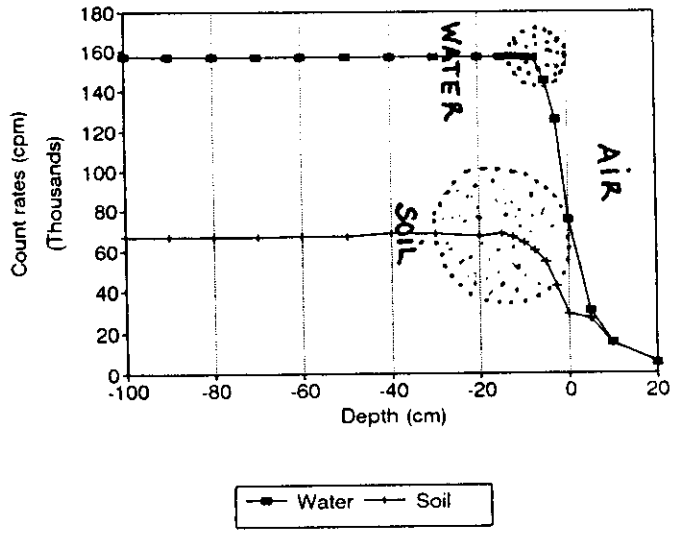

Figure 5. Spheres of influence in soil and water.

Table 3. Count rate as a function of depth (counted from soil surface) for two homogeneous media: water and soil with $\Theta = 0.35\ cm^3/cm^3$.

dept (cm)	count rate (cpm)	
	water	soil
100	157,230	67,100
90	157,110	67,030
80	157,130	66,880
70	157,020	66,950
60	156,890	67,230
50	157,150	67,310
40	156,970	68,910
30	157,080	68,370
20	157,160	67,250
15	157,020	68,630
12,5	157,240	66,870
10	157,000	64,150
7,5	156,540	59,800
5	145,230	54,360
2.5	125,810	42,550
0	75,440	29,120
+ 5	30,770	26,670
+10	15,300	14,590
+20	5,110	5,670

7. ERROR ANALYSIS

Figure 6 shows schematically a depth neutron probe, in a measurement position. The "active" center of measurement is located at a point A, depth z (cm) measured from soil surface. If a soil water content Θ ($cm^3.cm^{-3}$) measurement is made at this point, several sources of error contribute to the final result. These are (without priority):

a) counting time T (min)
a_1) for soil measurement T_c (min)
a_2) for standard measurement T_s (min)

b) calibration

c) instrument performance

d) position of active center

e) sphere of influence of slow neutrons
e_1) effect of diameter
e_2) effect of proximity of soil surface
f) access tube installation

g) relative location in the field

h) ohters

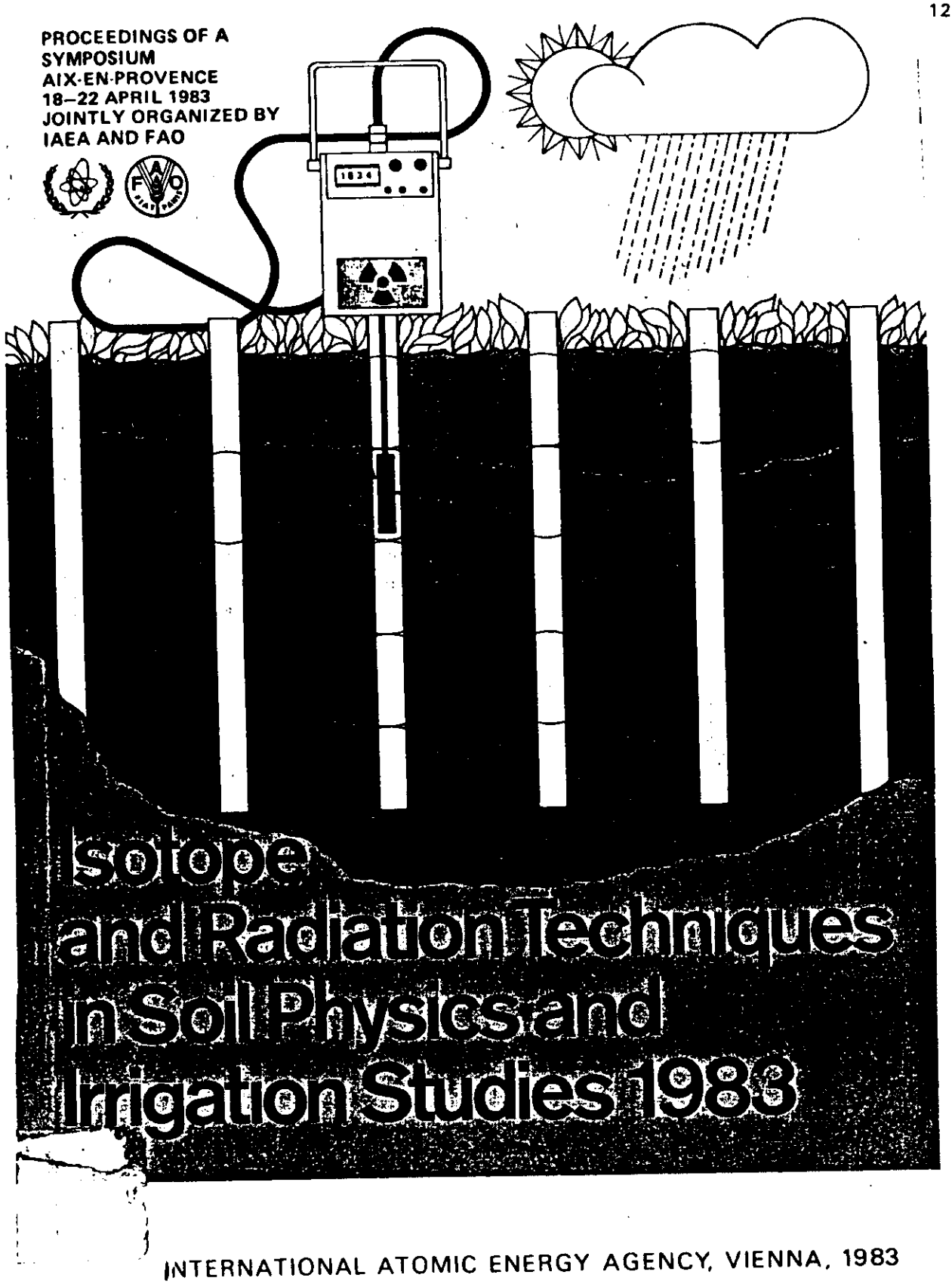

Figure 6. Neutron proble at measuring position A, depth z.

Some of these sources of error are inter-related and an analysis can only be made in a global form . We will discuss them separately as much as possible, but our final error analysis will lump some together or even neglect some.

Conting time errors arise due to the phisical processes by which neutrons are produced by the radioactive source, by which they are diffused and slowed down in the medium and by which they are detected. Here is an overlaping with **instrument performance**, due to geometry of the probe, source strength, electronics, etc. For a matter of simplicity, the whole counting process is assumed to follow Poisson's distribution (mostly the neutron emission process does), and therefore in a general sense, the longer we count, the smaller the standard deviations of the measurements. In practice, however, counting times greater than 5 minutes are seldomly used. The most common counting times T_c are I or 0.5 min. For the standard count T_s it is common to use longer times, from 3 to 5 minutes, since it is nade only once, before going to the field.

During calibration other errors are added, these being mainly associated to regression errors and to the "quality" of the Θ, CR values used to establish the calibration curve.

Once calibrated, the neutron probe can be used in water content measurements using different access-tubes, what introduces new errors due to soil spatial variability. These errors we will call **"local errors"**.

New errors are introduced when calculating soil water storages, which envolve the integration of Θ values in the soil profile. In this manuscript we will detail the errors of the Trapezoidal and of Simpson's methods of integration.

7.I. Instrumental and calibration errors

Based on Table 2 data it is possible to construct Table 4, which has the information needed to establish the equation of the linear regression between Θ and CR, which will be the calibration curve.

TABLE 4 - Values of Θ and CR, and calculations needed for the establishment of the calibration curve.

N°	Θ	CR	Θ x CR	CR^2	Θ^2	$(CR-\overline{CR})^2$	$(\Theta-\bar{\Theta})^2$
I	0.42400	0.50700	0.2I497	0.25705	0.I7978	0.005806	0.004942
2	0.4I300	0.48I00	0.I9865	0.23I36	0.I7057	0.002520	0.003516
3	0.39300	0.48500	0.I906I	0.23523	0.I5445	0.002938	0.001544
4	0.38700	0.45300	0.I753I	0.2052I	0.I4977	0.000493	0.001108
5	0.37800	0.43200	0.I6330	0.I8662	0.I4288	0.000001	0.000590
6	0.37500	0.44I00	0.I6538	0.I9448	0.I4063	0.000104	0.000453
7	0.30600	0.37700	0.II536	0.I42I3	0.09364	0.002894	0.002275
8	0.28700	0.36700	0.I0533	0.I3469	0.08237	0.004070	0.004448
9	0.29I00	0.39500	0.II495	0.I5603	0.08468	0.001282	0.003931
I0	0.28300	0.37000	0.I047I	0.I3690	0.08009	0.003697	0.004998
Σ	3.5370	4.3080	I.5486	I.8797	I.2788	0.023806	0.027810

C_s = I57,050 cpm (count rate in water)

$\bar{\theta}$ = 0.3537 cm^3/cm^3 CR = 0.4308 cpm n = I0

Calculation of the regression $\theta = a + b.CR$

$$a = \frac{(\Sigma\ CR^2)\ .\ (\Sigma\ \theta)\ -\ (\Sigma\ CR)\ .\ (\Sigma\ CR.\theta)}{n\ .\ \Sigma\ CR^2\ -\ (\Sigma\ CR^2)} \qquad (6)$$

or

$$a = \frac{\Sigma\,\theta}{n} - b \cdot \frac{\Sigma\,CR}{n} \tag{7}$$

$$b = \frac{n\,\Sigma\,CR.\theta - (\Sigma\,CR) \cdot (\Sigma\,\theta)}{n\,\Sigma\,CR^2 - (\Sigma\,CR)^2} \tag{8}$$

$$r = \frac{\Sigma\,CR \cdot \theta - \frac{(\Sigma\,CR) \cdot (\Sigma\,\theta)}{n}}{\sqrt{\left[\Sigma\,CR^2 - \frac{(\Sigma\,CR)^2}{n}\right]\left[\Sigma\,\theta^2 - \frac{(\Sigma\,\theta)^2}{n}\right]}} \tag{9}$$

$$r = \frac{Cov\,(x\,,\,y)}{\sqrt{V(x) \cdot V(y)}} \tag{10}$$

Results: Using the respective values of Table 4 in the above equations, the following results are obtained: (results of Table 5 are the out put of the linear regression program of LOTUS).

Table 5. Results of the linear regression of Table 4 data, using the LOTUS program.

Regression Output:		
Constant	-0.09535	(a = intersept)
Std Err of Y Est	0.015589	
R Squared	0.930091	
N° of Observations	10 (n)	
Degress of Freedom	8	
X Coefficient(s)	1.042376	(b = Slope)
Std Err of Coef.	0.101036	s^2 (CR)

The regression equation of the calibration curve of this probe for this soil depth is, therefore:

$$\theta = -\,0.09535 + 1.042376 \cdot \hat{CR}$$

where $\hat{\theta}$ and $\hat{CR}$ are estimatives of θ and CR.

Analysis of Variances:

For the case in question, the following variance analysis can be performed (Table 6):

Table 6. Analysis of Variance related to Table 5 data.

Causes of variation	DF	SQ	MS	F
Regression	1	0.025865	0.025865	106.4359
Residue	8	0.001944	0.000243	
Total	9	0.027810		

DF: degress of freedom
SQ: sum of squares
MS: mean of squares
F : test

The values presented in Table 6 are calculated according to:

$$SQtotal = \Sigma\, \theta^2 - \frac{(\Sigma\, \theta)^2}{n} \tag{11}$$

$$SQregression = \frac{\left[\sum (\theta.CR) - \frac{(\sum \theta \cdot \sum CR)}{n}\right]^2}{\left[\sum CR^2 - \frac{(\sum CR)^2}{n}\right]} \tag{12}$$

$$SQresidue = SQtotal - SQregression$$

Correlation significance tests:

t Test

$$t = \frac{r\sqrt{n-2}}{\sqrt{1-r^2}} \tag{13}$$

For the present case we have:

t = 5.05 (0.1%)
t = 10.32*** > t table for n = 8) t = 3.36 (1.0%)
t = 2.31 (5.0%)

F Test:

$$F = \frac{MS\ regression}{MS\ residue} = \frac{SQ\ regr./n^o.of\ degl.\ freedom.regr.}{SQ\ resid./n^o.of\ degl.freed.resisd.}$$

and for the present care:

$$F = \frac{0.025865}{0.000243} = 106.4359^{**} > (table) = 11.26$$

(*degress of freedom* 1 =*reg*, 8 *res.*)

As can be seen, both t and F tests were highly significant, indicating that the correlation coefficient r strongly differs from zero.

7.1.1. Variances and covariances (Cov) of the estimatives of the parameters and of the regression

$$s^2(\hat{b}) = \frac{MSres}{\Sigma\,(CR - \overline{CR})^2} = \frac{0.000243}{0.023806} = 0.010208 \quad (14)$$

$$s^2(\hat{a}) = [\frac{1}{n} + \frac{\overline{CR}^2}{\Sigma(CR - \overline{CR})^2}]\ MSres = 0.001918 \quad (15)$$

$$Cov(\hat{a}, \hat{b}) = s(\hat{a}, \hat{b}) = \frac{(\overline{CR}\ .\ MSres)}{\Sigma\,(CR - \overline{CR})^2} + 0.00439 \quad (16)$$

7.1.2. Total variance of θ

The regression equation obtained above contains estimated values of the real values of θ, CR, a and b, indicated by θ CR, $\hat{a}$ and b, respectively. So we have:

$$\hat{\theta} = \hat{a} + \hat{b}\ \hat{CR}\ (estimative) \quad (17)$$

$$\theta = a + b\ CR + e_o\ (true) \quad (18)$$

where: $E(\hat{a}) = a$ and $\hat{E}(b) = b$ (expectations).

The difference between a true θ value and its estimative, is given by:

$$\theta - \hat{\theta} = a - \hat{a} + bCR - \hat{b}\hat{CR} + e_o$$

or, in another form:

$$\theta - \hat{\theta} = a - \hat{a} + \hat{b}\ (CR - \hat{CR}) + CR\ (b - \hat{b}) + e_o \quad (19)$$

The mathematical expectation of the square of the difference will be:

$$E\{(\theta-\hat{\theta})^2\} = E\{(a-\hat{a})^2\} + E\{\hat{b}^2(CR-\hat{CR})^2\}+E \quad (20)$$

$$\{CR^2(b - \hat{b})^2\} + E(e_o^2) + 2.E\{CR\ (a - \hat{a})(b - \hat{b})\}$$

Equation (20) can be writhen as follows:

$$s^2(\hat{\theta}) = s^2(\hat{a}) + [\hat{b}^2 + s^2(\hat{b})].s^2(\hat{C}\ R + \quad (21)$$

$$\hat{CR}^2 s^2(\hat{b}) + s^2(e_o) + 2.\ \hat{CR}\ (\hat{a},\hat{b})$$

The variance $s^2(\hat{C}\overline{R})$ can be estimated from:

where $\hat{N}$ and N_s are the counting rates in the soil and in the

$$s^2(\hat{C}\,\overline{R}) = \left(\frac{\hat{N}}{\hat{N}_s}\right)^2 \left(\frac{s^2(\hat{N})}{\hat{N}^2} + \frac{s^2(\hat{N}_s)}{\hat{N}_s^2}\right) \tag{22}$$

standard, obtained during choosen comting times T and T_s, respectively. Considering that the neutron emission process follows

Poisson's Distribution, the variances associated to N and N_s are:

$$s^2(N) = \frac{1}{P}\,\frac{\hat{N}}{T} \tag{23}$$

$$s^2(\hat{N}_s) = \frac{1}{q}\,\frac{\hat{N}_s}{T_s} \tag{24}$$

where p and q are the numbers of replicates of counts made in the soil and in the standard, respectively.

Substituting 23 and 24 into 22, we have:

$$s^2\,(\hat{C}\overline{R}) = \left(\frac{\hat{C}R}{p.T} + \frac{\hat{C}R^2}{q.T_s}\right) + \hat{N}_s \tag{25}$$

and substituting 25 into 21:

$$s^2(\hat{\theta}) = [\hat{b}^2 - s^2(\hat{b})].\left[\frac{\hat{C}R}{p.T} + \frac{\hat{C}R^2}{q.T_s}\right]\frac{1}{\hat{N}_s} + s^2(\hat{a}) + s^2(\hat{b})\hat{C}R^2 + 2.\hat{C}RS(\hat{a},\hat{b}) + s^2(e_o) \tag{26}$$

which is the general equation for the total variance of the estimated soil water content. This equation is composed of two parts:

a) Variance due to calibration:

$$s_c^2(\hat{\theta}) = s^2(\hat{a}) + s^2(\hat{b})\;\hat{C}R^2 + 2.\hat{C}RS\;(\hat{a},\hat{b}) + s^2(e_o) \tag{27}$$

b) Variance due to instrmental error:

$$s_i^2(\hat{\theta}) = [\hat{b}^2 - s^2(\hat{b})]\;\left[\frac{\hat{C}R}{p.T} + \frac{\hat{C}R^2}{q.T_s}\right].\;\frac{1}{\hat{N}_s} \tag{28}$$

Example: To calculate $s^2_c(\theta)$ and $s^2_i(\theta)$, we need the parameters $\hat{a}$ and $\hat{b}$, and their variances and covariances. We also need a set of neutron probe measurements at one location (same access tube) and at one choosen depth. To calculate CR (estimated mean value) we also need standard measurements. Table 7 gives us an example:

Table 7. Neutron probe data for z = 60 cm, collected at one access tube installed in "terra roxa estruturada" soil, with 5 replicates. Standard measurement made in water.

Replicates	Counts (C)	T	$\hat{N}$ (cpm)	$\hat{CR}$
1	140800	2	70400	0.444
2	138200	2	69100	0.436
3	140500	2	70250	0.443
4	139900	2	69950	0.441
5	139100	2	69950	0.439
Mean	139700	2	69850	0.4406
Standard (Water)	317000 (C)	2 (Ts)	158500 (Ns)	

Using equations 23, 24 and 22, we have:

$$s^2(\hat{N}) = \frac{1}{5}\,\frac{69850}{2} = 6985$$

$$s^2(\hat{N}_s) = \frac{1}{1}\,\frac{158500}{2} = 79250$$

$$s^2(\hat{C}\ \overline{R}) = \left(\frac{69850}{158500}\right)^2 \left(\frac{6985}{69850^2} + \frac{79250}{158500^2}\right) = 8.9 \cdot 10^{-7}$$

It is important to observe that increasing the number of replicates p and q, as well as the counting times T and T_s, the variances will decrease. One count for a longer time has the same effect than increasing the number of replicates.

Using equations 27 and 28 we now calculate the calibration and the instrumental variances of the soil water content $\hat{\theta} = \{-0.09535 + 1.042376 \times 0.4406\} = 0.364\ cm^3.cm^{-3}$, which corresponds to the measured value of CR = 0.4406:

a) Calibration Variance

$$s^2_c(\theta^*) = 0.001918 + 0.010208 \cdot 0.4406^2 + 2 \times 0.4406 \cdot (-0.00439) + s^2(\theta_o)$$

where

$$s^2(\theta_o) = MSres = 0.000243$$

and, therefore:

$$s_o^2(\theta^*) = 2.74 \times 10^{-4}$$

The standard deviation of $\hat{\theta}$ due to calibration is:

$$s_o(\hat{\theta}) = \sqrt{2.74 \cdot 10^{-4}} = 1.66 \cdot 10^{-2}$$

with a coefficient of variation of:

$$CV\% = \frac{s_o(\bar{\hat{\theta}})}{\hat{\theta}} = \frac{1.66 \cdot 10^{-2}}{0.3639} = 4.5\%$$

b) Instrumental Variance

$$s_I^2(\bar{\hat{\theta}}) = (1.042376^2 - 0.010208)\left(\frac{0.4406}{5 \times 2} + \frac{0.4406^2}{1 \times 2}\right)\frac{1}{158500}$$

$$s_I^2(\bar{\hat{\theta}}) = 5.98 \cdot 10^{-7}$$

and

$$s_I(\bar{\hat{\theta}}) = \sqrt{9.58 \cdot 10^{-7}} = 9.79 \cdot 10^{-4}$$

$$CV\% = \frac{9.79 \cdot 10^{-4}}{0.3639} = 0.27\%$$

c) Total variance

$$s^2(\bar{\hat{\theta}}) = s_c^2(\theta) + s_I^2(\theta^*) = 2.74 \times 10^{-4} + 0.00958 \cdot 10^{-4} = 2.75 \times 10^{-4}$$

and so:

$$s(\bar{\hat{\theta}}) = \sqrt{2.75 \cdot 10^{-4}} = 1.66 \times 10^{-2}$$

$$CV\% = \frac{1.66 \times 10^{-2}}{0.3639} = 4.56\%$$

These results show that calibration errors are much more important than instrumental errors. Any attempt to decrease the total variance should focus the calibration procedure.

It is important to remind the reader that the above analysis is valid for one neutron access tube at one choosen depth. We will now study the variance of several measurements performed at different access tubes, at one choosen depth.

7.2. Local Error: (Havercamp et al. 1984 and Vauclin et al 1984).

Measuring soil water content with replicates of CR obtained in different access tubes scattered randomly in a field, we obtain a mean value $<\hat{\theta}>$ which has one more variance component, corresponding to the spatial variability of the soil in the field.

The variance due to the position of the measurement in the field (VAUCLIN et al. 1984) is given by:

$$s_L^2(\overline{<\hat{\theta}>}) = [\hat{b}^2 - s^2(\hat{b})] \cdot \frac{s^2(L)}{k\hat{N}s} \tag{29}$$

where $s^2(L)$ is the soil spatial variability variance.

Due to the difficulties envolved in the determination of $s^2(L)$ these authors suggest that $s^2_L(<\Theta>)$ should be calculated by difference, according to:

$$s_L^2(<\bar{\hat{\theta}}>) = s^2(<\bar{\hat{\theta}}>) - s_o^2(<\bar{\hat{\theta}}>) - s_i^2(<\bar{\hat{\theta}}>) \tag{30}$$

in which, by analogy to equation 21, $s^2(<\theta>)$ is given by:

$$s^2(<\bar{\hat{\theta}}>) = [\hat{b}^2 + s^2(\hat{b})]\, s^2(<\overline{\hat{CR}}>) + s^2(\hat{a}) + (<\hat{CR}>)^2 s^2(\hat{b}) + 2<\overline{\hat{CR}}>\, s(a,b) + \underline{s^2(e_o)} \tag{31}$$

In equation 31, $s^2(e_o) = MS_{res} = 0$ because it is the variance of a mean value. In this equation $s^2(<\hat{CR}>)$ accounts for local variability:

$$s^2(<\overline{\hat{CR}}>) = \frac{1}{k}\, s^2(\hat{CR}) \tag{32}$$

where $1/k\ s^2(CR)$ represents the mean of the variance of k measurements of CR performed in k access tubes, at a same depth.

Exemple: Table 8 shows CR values from a set of 30 access tubes of a "homogeneous" field, at the depth of 40 cm. As an example we take five measurements (k = 5), corresponding to access tubes 6, 14, 26, 29 and 30, shown in Table 8a.

Table 8. CR data for 30 neutron access tubes instaled in "terra roxa estruturada", at the depth of 40 cm.

Access tube n°	CR	Access tube n°	CR
1	0.476	16	0.464
2	0.507	17	0.511
3	0.508	18	0.49
4	0.515	19	0.488
5	0.515	20	0.486
6	0.535	21	0.489
7	0.528	22	0.497
8	0.513	23	0.479
9	0.494	24	0.467
10	0.504	25	0.485
11	0.469	26	0.452
12	0.497	27	0.487
13	0.484	28	0.485
14	0.487	29	0.478
15	0.477	30	0.475
		$<\hat{CR}>$ =	0.4914

T = 1 q = 1 Ns = 1020 (water)
Ts = 1

Table 8a. Data for five access tubes choosen randonly from Table 8.

Access tube n°	$\hat{CR}$	$(\hat{CR} - <\hat{cR}>)^2$
6	0.535	2.46×10^{-3}
14	0.487	2.56×10^{-6}
26	0.452	1.12×10^{-3}
29	0.478	5.48×10^{-5}
30	0,475	$1,08 \times 10^{-4}$
	Σ =	3.74×10^{-3}

$$s^2(CR) = \frac{\sum[CR - \hat{CR}]^2}{k} = \frac{3.74 \times 10^{-3}}{5} = 7.48 \times 10^{4}$$

$$s^2(<\hat{CR}>) = \frac{1}{5} 7.48 \times 10^{-4} = 1.49 \times 10^{-4}$$

Total variance of soil water content:

$$s^2 = (<\bar{\hat{\theta}}>) = 22.2 \times 10^{-6} = (equation 31)$$

Instrumental variance:

$$s_i^2(<\bar{\hat{\theta}}>) = 0.228 \times 10^{-6} \quad (equation\ 28)$$

Calibration variance:

$$s_c^2(<\bar{\hat{\theta}}>) = 6.12 \times 10^{-6} \ [equation\ 27\ without\ \underline{s^2(e_o)}]$$

Spatial variability variance:

$$s_L^2(<\bar{\hat{\theta}}>) = 15.9 \times 10^{-6} \quad (equation\ 30)$$

If the above calculations are repeated for different sets of measurements, varying k, it will be observed that the instrumental variance is always very small when compared to the other, and that the calibration variance is fairly constant because it is not affected by k. On the other hand, the local variance s^2_L ($<\Theta>$) will decrease with the increase of observation points (k). For high values of k this effect levels off, as can be seen in Table 9 and Figure 6a. It is therefore possible to define the ideal number of access tubes (k) to be within a choosen coefficient of variation.

As an examle, for the 30 measurements of Table 8, $<CR>$ = 0.4914, corresponds to an estimated soil water content value of: $<\hat{\Theta}>$ = 0.4169 and since 30 is a high value of k, we consider this $<\Theta>$ value as being the true soil water content. Now, if we would like to measure this water content with a CV of 3%, how many access tubes do we need?

$$CV\% = \frac{s(<\bar{\hat{\theta}}>)}{<\bar{\hat{\theta}}>} \cdot 100$$

$$s<\bar{\hat{\theta}}> = \frac{3 \times 0.4169}{100} = 0.0125$$

therefore:

$$s^2<\bar{\hat{\theta}}> = 15.6 \times 10^{-6}$$

From Table 9 we can see that for this $s^2<\Theta>$, k would be between 5 and 10. Refining data of Table 9 for more values of k, we conclude that k should be of the order of 6 access tubes.

Table 9. Variance component behaviour as a function of the number of access tubes (k), using data of Table 8.

k	access tube n°	$s^2(\hat{ER})$ (x 10^{-4})	$s^2(<\hat{\Theta}>)$ (x 10^{-5})	$s^2_i(<\hat{\Theta}>)$ (x 10^{-6})	$s^2_c(<\hat{\Theta}>)$ (x 10^{-5})	$s^2_t(<\hat{\Theta}>)$ (x 10^{-5})
5	6, 14, 26, 29 e 30	7.48	22.2	2.28	6.12	15.9
10	4, 5, 9, 15, 20, 23, 24, 26, 30	3.72	9.86	1.93	5.81	3.86
15	2, 3, 5, 7, 8, 8, 10, 12, 16, 18, 19, 24, 27, 28, 30	3.06	9.48	1.90	7.27	2.02
20	1, 2, 3, 5, 6, 9, 11, 13, 14, 15, 16, 17, 18, 19, 20, 22, 23, 26, 28	3.76	6.82	1.82	6.80	1.84
25	all less n°s 1, 3, 13, 15, 28	3.91	8.67	1.80	6.99	1.50
30	all	3.54	8.12	1.77	6.85	1.09

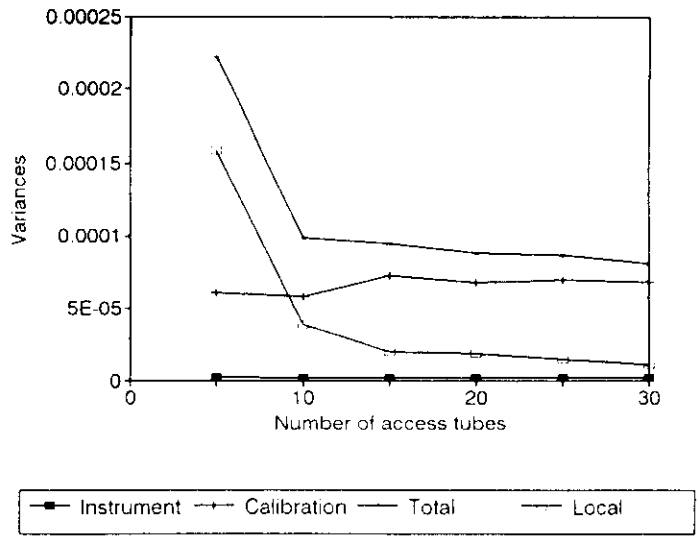

Figure 6a. Variance component behaviour as a function of the number of access tubes (k). Data of Table 9.

7.3. Errors of soil water storage calcualtion:

For soil water storage calculations, soil water contents are integrated from soil surface down to a desired depth. Therefore, the calculated storage will present errors due to Θ measurements and due to the integration method. Soil water storage at a fixed time is given by:

$$S_L = \int_0^L \theta(z)\, dz \tag{33}$$

and since the function Θ(z) is not known analitically, S_L is calculate numerically. The most frequently methods used are the Trapezoidal and Simpson's. In any case the total variance of soil water storage will be composed of the soil water content variance

$[s^2_1 (\hat{S}_L)]$ and the integration variance $[s^2_2 (\hat{S}_L)]$:

$$s^2(\hat{L}) = s_1^2(\hat{S}_L) + s_x^2(\hat{S}) \tag{34}$$

7.3.1. Trapezoidal Method:

Figure 7 shows a soil water profile for which we will calculate S_L.

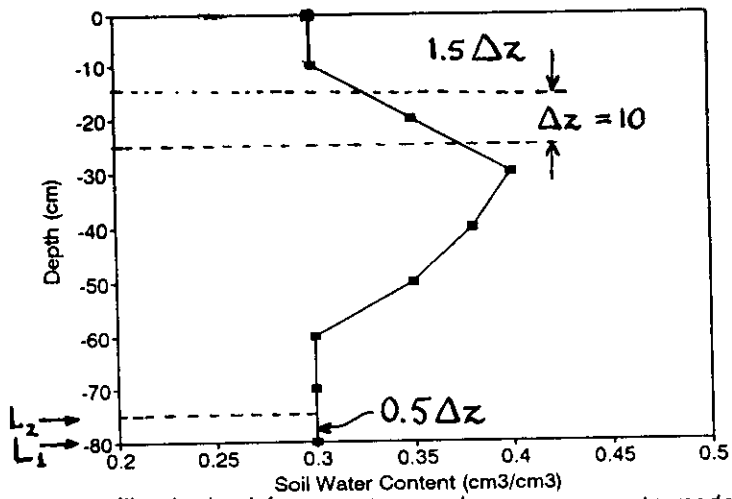

Figure 7. Soil water content profile obtained from neutron probe measurements made at 10 cm depth intervals.

Using the trapezoidal rule, the integral of equation (33) is approximated by:

$$\hat{S}_L = \int_0^z \theta\, d_z = \sum \theta_i \Delta z \tag{35}$$

If the estimative of S_L is made from 0 to L_1 (see Fig. 7) we have:

$$\hat{S}_{L1} = (1.5\theta_1 + 1\theta_2 + 1\theta_3 + \ldots + 0.5\theta_8)\Delta_z \quad (35\ a)$$

and if it is made down to L_2

$$\hat{S}_{L2} = (1.5\theta_1 + 1\theta_2 + 1\theta_3 + \ldots + 1\theta_7)\ \Delta_z \quad (35\ b)$$

The factor 1.5 stands for the fact that we do not have a suface measurement. In this example θ_1 was measured too close to soil surface. We will neglect this error. Using the variance properties we have:

$$s_1^2(\hat{S}_{L2}) = [1.5^2 s^2(\theta_1) + s^2(\theta_2) + s^2(\theta_3) + \ldots 0.5^2 s^2(\theta_8)]\Delta_z^2 \quad (36)$$

$$s_1^2(\hat{S}_{L1}) = [1.5^2 s^2(\theta_1) + \sum s^2(\theta_i)]\Delta_z^2 \quad (36\ a)$$

On the other hand, the variance of the Trapezoidal method is given by (CARNAHAN et al 1969):

$$s_2^2(\hat{S}_L) = \frac{L^2\Delta_z^4}{144}(\theta''(z))^2 \quad (37)$$

where $\Theta''(z)$ is the second derivative of $\Theta(z)$, which can be approximated by finite differences using Taylor's series:

$$s_2^2(\hat{S}_L) = \frac{L^2\Delta_z^4}{144}\left\{\frac{\theta_{i+1} - 2\theta_i + \theta_{i-1}}{\Delta z^2}\right\} \quad (38)$$

The second derivative has to be taken at all possible depths z_i, and for safety we use the largest obtained value for equation 38.

7.3.2. Simpson's Method:

For Simpson's method soil water storage is calculated as follows (CARNAHAN et al. 1969):

$$\hat{S}_L = \int_0^L \theta(z)\,dz = \frac{\Delta_z}{3}[\theta(z_0) + 4\theta(z_1) + 2\theta(z_2) + 4\theta(z_3) + 2\theta(z_4) + \ldots + 2\theta(z_{2n-2}) + 4\theta(z_{2n-1}) + \theta(z_n)] - \frac{\Delta_z^5}{90}\sum_{i=1}^{n}\theta''''(z) \quad (39)$$

2 n = n° of soil layers
where: n = n° of 4th order derivatives

Using the variance properties:

$$s_1^2(S_i) = \left(\frac{\Delta_z}{3}\right)^2 [s^2(\theta_0) + 4^2 s^2(\theta_1) + 2^2 s^2(\theta_2) + 4^2 s_2(\theta_3) + 2^2 s^2(\theta_4) + \ldots$$

$$+ 2^2 s^2(\theta_{2n-2}) - 4^2 s^2(\theta_{2n-1}) + s^2(\theta_{2n})] \quad (40)$$

The variance of Simpson's integration method is given by

$$s_2^2(\hat{A}) = \frac{L^2 . \Delta_z^8 [\theta''''(z)]^2}{32400} \quad (41)$$

where Θ""(z) is the fourth derivative of Θz), which can also be estimated by finite differences:

$$s_2^2(\hat{S}_i) = \frac{L^2 \Delta_z^8}{32400} \left(\frac{\theta_{i+2} - 4\theta_{i+1} + 6\theta_i - 4\theta_{i-1} + \theta_{i-2}}{4! \Delta_z^4} \right)^2 \quad (42)$$

Example: Table 10 presents soil water content data measured with the same probe, in 25 cm depth increments, down to 150 cm, at 25 locations (access tubes). For the trapezoidal method we have:

$$\overline{\hat{S}} = (1.5 \times 0.336 + 0.347 + 0.325 + 0.300 + 0.296 + 0.5 \times 0.297)$$
$$\times 25 = 47.99 \text{ cm} = 479.9 \text{ mm}$$

$$s_1^2(\hat{S}_{150}) = [1.5^2 \times 0.00086 + 0.00106 + 0.00031 + 0.00019 +$$

$$0.00030 + 0.5 \times 0.00028] = 2.41 \text{ cm}^2 \quad (eq.\ 36)$$

$$s_1(\hat{S}_{150}) = \sqrt{2.41} = 1,55 \text{ cm} = 15,5 \text{ mm}$$

$$s_2^2(\hat{A}) = \frac{150^2 . 25^4}{144} [\theta''(z)]^2 \quad (eq.37)$$

and

$$1 - \theta''(z) \text{ at } 50 \text{ cm} = \frac{0.325 - 2 \times 0.347 + 0.336}{25^2} = -5.3 \cdot 10^{-6}$$

$$2 - \theta''(z) \text{at } 75 \text{ cm} = \frac{0.300 - 2 \times 0.325 + 0.347}{25^2} = -4.7 \cdot 10^{-6}$$

$$3 - \theta''(z) \text{at } 100 \text{ cm} = \frac{0.296 - 2 \times 0.300 + 0.325}{25^2} = +3.3 \cdot 10^{-6}$$

$$4 - \theta''(z) \text{at } 125 \text{ cm} = \frac{0.297 - 2 \times 0.296 + 0.300}{25^2} = +8.0 \cdot 10^{-6}$$

The largest value in absolute terms of $\Theta''(z)$ is for z = 50 cm, therefore:

$$s_2^2(\hat{S}_{150}) = \frac{150^2 \times 25^4}{144} [-5.3 \times 10^{-5}]^2 = 1.7 \times 10^{-1} \text{ cm}^2$$

and the standard deviation will be:

$$s_2(\hat{S}_{150}) = \sqrt{1.7 \cdot 10_{-1}} = 0.4123 \text{ cm} = 4.12 \text{ mm}$$

and finally:

$$s^2(\hat{S}_{150}) = s_1^2(\hat{S}_{150}) + s_2^2(\hat{S}_{150}) = 2.58 \text{ cm}^2 \qquad (eq.34)$$

$$s(\hat{S}_{150}) = \sqrt{2.58} = 1,606 \text{ cm} = 16.06 \text{ mm}$$

2. Simpson's Method:

$$\hat{S}_L = \frac{25}{3} [0.336 + 4 \times 0.336 + 2 \times 0.347$$

$$+ 4 \times 0.325 + 2 \times 0.300 + 4 \times 0.296 + 0.297] \qquad (eq.39)$$

The water content at z_o is taken equal to that of z_1, because it was not measured.

$$\hat{S}_L = 47.93 \text{ cm} = 479.3 \text{ mm}$$

which is essentially the same value obtained by the trapezoidal rule.

$$s_1^2(\hat{S}_{150}) = \left(\frac{25}{3}\right)^2 \{0.00086 + 4^2 \times 0.00086 + 2^2 \times 0.00106 + 4^2 \times 0.00031 +$$

$$+ 2^2 \times 0.00019 + 4^2 \times 0.00030 + 0.00028 \} = 2.06\ cm^2 \qquad (eq.40)$$

and

$$s_1(\hat{S}_{150}) = \sqrt{2.06} = 1.435\ cm = 14.35\ mm$$

$$s_2^2(\hat{S}_{150}) = \frac{150^2 \times 25^8}{32400} [\theta''''(z)]^2 \qquad (eq.41)$$

and

$$1 - \theta''''(z) at 50\ cm = \frac{0.300 - 4x0.325 + 6x0.347 - 4x0.336 + 0.336}{41\ 25^4}$$

$$2 - \theta''''(z) at\ 75\ cm = \frac{0.296 - 4x0.300 + 6x0.325 - 4x0.347 + 0.336}{41\ 25^4}$$

$$3 - \theta''''(z) at\ 100\ cm = \frac{0.297 - 4x0.296 + 6x0.300 - 4x0.325 + 0.347}{41\ 25^4}$$

Since the highest value corresponds to z = 50 cm, $\Theta''''(z) = 7.89 \times 10^9$, we use this one.

$$s_2^2(\hat{S}_{150}) = \frac{150^2 \cdot 25^8}{32400} \cdot (7.89 \times 10^{-9})^2 = 6{,}59 \times 10^{-6}$$

and the standard deviation will be:

$$s_2(\hat{S}_{150}) = 2{,}57 \times 10^{-3}\ cm^2 = 0.026\ mm$$

finally:

$$s^2(\hat{S}_{150}) = s_1^2(\hat{S}_{150}) + s_2^2(\hat{S}_{150}) = 2.06 + 2.57 \times 10^{-3} = 2.06$$

$$s(\hat{S}_{150}) = 1.435\ cm = 14.35\ mm$$

All the above calculations can be summarized in:

Method	$\hat{S}_{150}$	$s^2_1(\hat{S}_{150})$	$s^2_2(\hat{S}_{150})$	$s^2(\hat{S}_{150})$	$s(\hat{S}_{150})$	C.V.
Trapezoidal	47.99	2.41	0.170	2.58	1.61	3.35%
Simpson	47.93	2.06	6.59×10^{-6}	2.06	1.43	2.98%

As can be seen, Simpson's method yields lower variances, mainly with respect to integration. However, the final result is just about the same since the coefficients of variation do not differ significantly. This is the reason why most people use the Trapezoidal Method. In either case it is important to observe that the main source of errors comes from the measurement of Θ, given by s^2_1 and not from the integration method, given by s^2_2.

Table 10. Soil water content data collected 22.10.90 on 25 access tubes installed in "terra roxa estruturada" soil, at Piracicaba, SP. Brasil.

Access tube	25 cm	50 cm	75 cm	100 cm	125 cm	150 cm
1	0.372	0.393	0.383	0.344	0.304	0.293
2	0.378	0.393	0.347	0.308	0.300	0.313
3	0.359	0.352	0.327	0.317	0.300	0.300
4	0.379	0.374	0.309	0.288	0.293	0.299
5	0.362	0.353	0.320	0.288	0.284	0.285
6	0.358	0.336	0.316	0.301	0.281	0.296
7	0.315	0.337	0.316	0.291	0.291	0.293
8	0.365	0.393	0.345	0.298	0.287	0.292
9	0.315	0.334	0.312	0.300	0.305	0.338
10	0.362	0.382	0.355	0.316	0.315	0.332
11	0.357	0.358	0.316	0.291	0.364	0.281
12	0.361	0.370	0.327	0.294	0.276	0.282
13	0.346	0.343	0.317	0.297	0.300	0.290
14	0.348	0.347	0.307	0.278	0.283	0.274
15	0.332	0.335	0.335	0.298	0.288	0.289
16	0.323	0.338	0.323	0.295	0.290	0.315
17	0.291	0.311	0.312	0.310	0.296	0.306
18	0.326	0.345	0.336	0.324	0.303	0.295
19	0.328	0.384	0.336	0.296	0.286	0.286
20	0.285	0.234	0.306	0.291	0.289	0.278
21	0.340	0.334	0.308	0.287	0.286	0.292
22	0.294	0.339	0.310	0.285	0.286	0.287
23	0.315	0.326	0.314	0.295	0.282	0.288
24	0.301	0.325	0.323	0.308	0.317	0.335
25	0.283	0.333	0.319	0.298	0.287	0.297
Mean	0.336	0.347	0.325	0.300	0.296	0.297
Variance	0.00086	0.00106	0.00031	0.00019	0.00030	0.0002

L = 150 cm $\quad \Delta_z$ = 25 cm

8. APLICATIONS

8.I. Soil Water Storages

The water stored in a soil layer at depths L_1 and L_2, at time t, is defined as:

$$S_{L2-L1}(t) = \int_{L_1}^{L_2} \theta \, dz \qquad (33\ b)$$

where Θ is the volumetric soil water content given by equation 2, and z is the vertical position coordinate, measured downwards from soil surface.

Using Θin cm^3 of water per cm^3 of soil, and z in cm, the result of S is a height of water, given in cm. Each cm of stored water corresponds to a volume of IO liters of water per square meter of soil surface, down to the integrated depth. The most common case is when $L_1 = 0$ (soil surface) and the integration is made over the whole soil profile, down to depth L_2.

As already seen in general the function Θ(z) that describes the variation of Θalong z is not known and it is necessary to use numerical schemes of integration. Havercamp et al. (I984) and Vauclin et al. (I984) discuss the use of the trapezoidal and simpson's rules. For most agronomical purpuses, the trapezoidal rule is very adequate and, therefore, our example will cover this case only.

According to the trapezoidal rule, equation (2I) is simplified to:

$$S_{L2-L1}(t) = \bar{\theta}\,(L_2 - L_1) \qquad (33\ c)$$

where Θ is the average value of Θin the interval $L_2 - L_1$.

Table 8 shows neutrons moisture data collected at an access tube installed in a corn field. The neutron probe is the same as the one used for the calibration example in Figure 3.

Table II. Count ratios and soil water contents as a function of depth, for a corn crop, on September 7, I988. Alfisol, Piracicaba, SP, Brasil.

Depth (cm)	Count Ratio (CR)	Soil Water Content ($cm^3.cm^{-3}$)
25	0.494	0.420
50	0.485	0.4I0
75	0.503	0.429
I00	0.473	0.398
I25	0.465	0.389
I50	0.47I	0.396

Using equation (33 c) it is easy to calculate the following soil water storages:

$$A_{0\text{-}150}\ (7/9/88) = 0.407\ (150 - 0) = 61.1\ cm = 611\ mm$$
$$A_{0\text{-}75}\ (7/9/88) = 0.420\ (75 - 0) = 31.5\ cm = 315\ mm$$
$$A_{50\text{-}100}\ (7/9/88) = 0.412\ (100 - 50) = 20.6\ cm = 206\ mm$$

As already discussed in item 6, it is important to know the "shere of influence" of the probe. This is specially true for the measurements close to soil surface. In the present case, the "sphere of influence" has a diameter of the order of 30 cm. This means that when the probe is placed at the depth of 25 cm, we are making a

measurement from 10 to 40 cm depth; so we are loosing the top 10 cm. This introduces an error in our storage calculations when they start at soil surface. On the other hand, it is good because we are sure that neutrons did not escape from soil surface, which also introduces errors. Therefore many times we take gravimetric samples at soil surface.

It is also important to note that the measurements of the probes are not punctual but, in actual fact, are averages over a soil layer of the thickness of the spere of influence. Figure 8 illustrates this for the data of Table 8. This fact has advantages when calculating soil water storages because, as shown by equation (33 c), the calculation is based on averages. Even the overlaping of spheres does no harm, on the contrary, it improves the sampling of the profile.

In our example, if measurements would have been taken in 10 cm intervals, the overlaping would be greater and the estimative of soil water storage, better. Attention must only be taken at soil surface. If we start measuring at the depth of 10 cm, part of the "sphere of influence" would be outside the soil.

Modern models of neutron probes have microprocessors that calculate automatically the soil water storage, giving results in mm of water, or inches per foot. Others, more sophysticated, move up and down in the access tube, at a constant speed, making an excellent integration of the soil water profile.

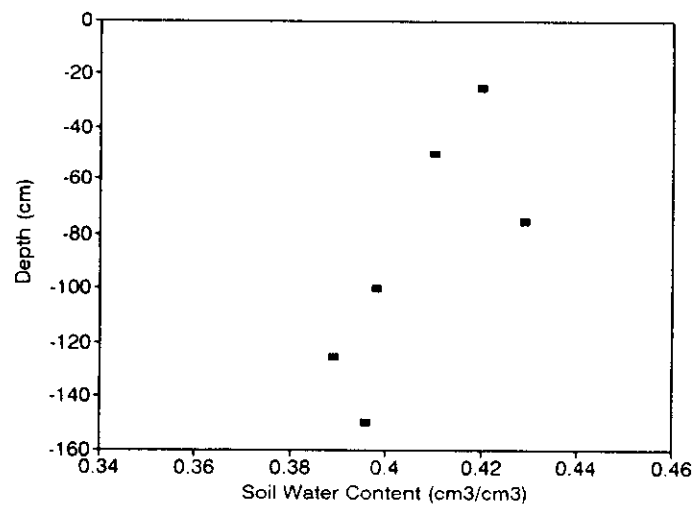

Figure 8. Soil water content profile in a corn crop (07/09/88).

Very important are also soil water content changes in time. As soil gains water by rainfall or irrigation, or as soil looses water by evapotranspiration or internal drainage, soil water storage changes in time. For the same corn crop illustrated in Table 8 and Figure 7, neutron probe measurements made at different dates gave the following storages:

$$A_{0-150}\ (14/9/88) = 579{,}5\ mm$$
$$A_{0-150}(21/9/88) = 543{,}8\ mm$$
$$A_{0-150}\ (28/9/88) = 575{,}8\ mm$$

From 7 to 21/9 there was no rain or irrigation. The average rates of water loss were:

$$\frac{\overline{\partial A}}{\partial t} = \frac{A_{0-150}(14/9) - A_{0-150}(7/9)}{14 - 7} = -4.5\ mm/day$$

$$\frac{\overline{\partial A}}{\partial t} = \frac{A_{0\text{-}15}(21/9) - A_{0\text{-}150}(14/9)}{21 - 14} = -5.1 \text{ mm/day}$$

It is however impossible to partition these losses into evapotranspiration and drainage below 150 cm. If the soil was at the beginning at field capacity, we can be sure that 100% of the losses were evapotranspiration. Above field capacity, this is not true and fair amounts of water can be lost by deep drainage.

In the period 21 to 28/9 there was rain, therefore soil water storage increased.

8.2. Field soil water retention curves

Combining neutron probe readings with tensiometer readings, at the same depth, it is possible to establish soil water retention curves, that is, relations Θ versus Ψ_m. Tensiometers should be installed as close as possible to neutron access tubes, but not within the "sphere of influence" of the probe, because the tensiometer cup, being full of water, can interfere significantly in the readings of the probe. A distance of 20-30 cm should be ideal to avoid the interference. In many soils, however, bulk densities and water contents may vary significantly over these short distances. This was observed by Greminger et al. (1985) and Villagrea et al. (1988) that obtained very scattered points in their field soil water retention curves due to soil spatial variability. IAEA (1984) also presents soil water retention curves obtained with tensiometers and neutron probes, for soils of several countries. Figures 9 and 10, below, are two examples of soil water retention curves obtained from neutron probe and tensiometer data.

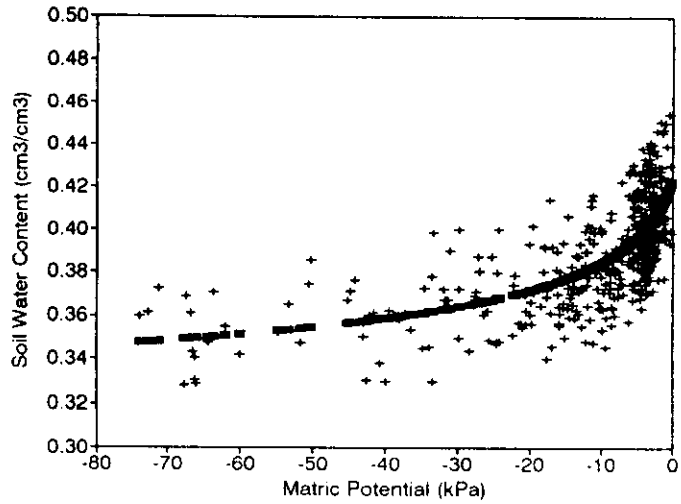

Figure 9. Soil water retention curve for "terra roxa estruturada", depth of 20 cm. Piracicaba. Brazil. Villagra et al (1988).

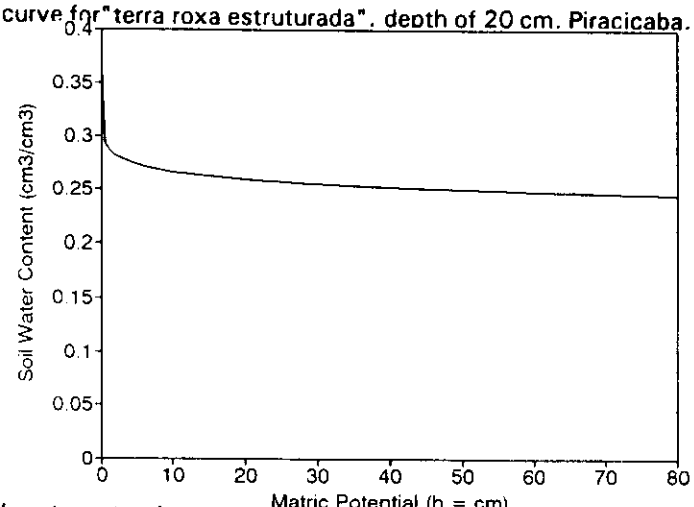

Figure 10. World average soil water retention curve (average of 11 countries over 6 depths). IAEA (1984).

8.3. Soil Hydraulic Conductivities

Soil hydraulic conductivity K being a parameter that indicates the hability of the soil in transmitting water, is strongly dependent on soil water contents (Θ). Therefore, for a given porous material we define the function K(Θ), and all methods used to measure hydraulic conductivity envolve the measurement of soil water contents. Among these methods several are adapted to use neutron probes, specially those developed for field conditions. As an example we will illustrate this section with one method presented by Libardi et al. (1980).

In a 5 x 5 mm plot, 3 to 5 neutron access tubes are installed down to the desired depth. Water is ponded until steady state infiltration. At this time neutron probe readings should be constant in time and indicate the saturated soil water contents of the profile. Steady state infiltration rate should also be recorded at surface, which is assumed to be the saturated hydraulic conductivity of the profile K_o.

After infiltration of the ponded water, soil surface is covered with plastic to avoid water evaporation, and internal drainage of the profile is observed through periodic soil water content measurements. Frequency of measurements is high at initial times (about twice a day) and becomes low as time passes (about twice a week), finishing the experiment after about one month. For these measurements neutron probes are extremely adequate because "same sites" are "sampled" each time of measurement. With auger techniques soil has to be uncovered each time and samplings are made every time at different locations. Auger holes disturb internal drainage process. During ponding and at early stages of infiltration, when soil is very wet and muddy it is impossible to sample soil with an auger.

Figure 11 shows plots of soil water content as a function of the natural logarithm of time, for two selected depths of a yellow-red latosol from Piracicaba, Brazil, measured with a SOLO 25 neutron probe. According to the procedure of Libardi et al. (1980), linear regressions of plots of Θ versus ℓ n t yield the coefficientes γ of the exponential K(Θ) relation:

$$K = K_o \exp [\gamma(\theta - \theta_d]$$

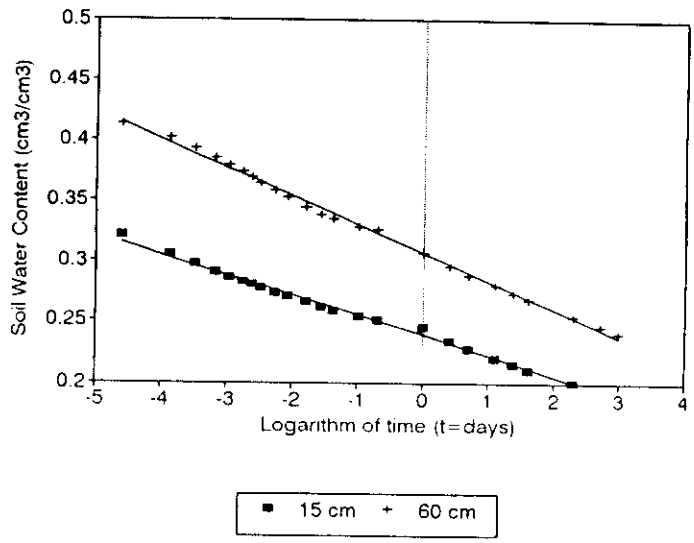

Figure 11. Plots of θ versus lnt, for two depths in a yellow-red latosol.

For the two examples of Figure 11the values of γ are 23.077 and 27.273, the value of K_o is 85.6 cm/day and the values of the saturated water content are 0.481 $cm^3.cm^{-3}$ and 0.439 $cm^3.cm^{-3}$. Therefore we have:

z = 50 cm $\quad K = 85.6 \exp [23.077(\theta - 0.450)]$

z = 150 cm $\quad K = 85.6 \exp [27.273 (\theta - 0.501)]$

8.4. Soil Spatial Variability

When the problem is to study spatial variability of soil water contents and better understand their variances, their dependence on space, etc, neutron probes are very suitable. These studies can be performed with advantages using the theory of regionalized variables and, in this context, a large number of sampling points is needed. Sampling schemes may be transects or grids, with points separated of constant lag h.

Figure 12 shows several neutron probe measurements of soil water contents, made over a transect of 25 access tubes, with a lag of 5 m, located in an Alfisol, Piracicaba, Brazil. The parallelism between curves of different days shows that the neutron probe really "samples" the same location at each time.

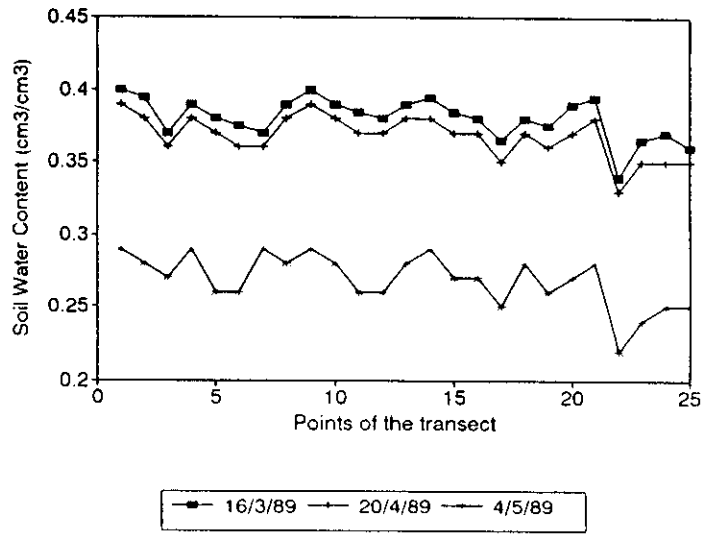

Figure 12. Soil water content measurements along a transecte of 25 points with lag of 5 m. Alfisol, Piracicaba, Brazil.

8.5. Water Extraction by Trees

In a rubber tree plantation tensiometer measurements of soil water potential Ψ_m and neutron probe measurements of soil water contentΘindicate patterns of soil water extraction (Figure 13). Measurements were made at several locations and at different depths so that it was possible to construct isolines of Ψ_m and Θ.

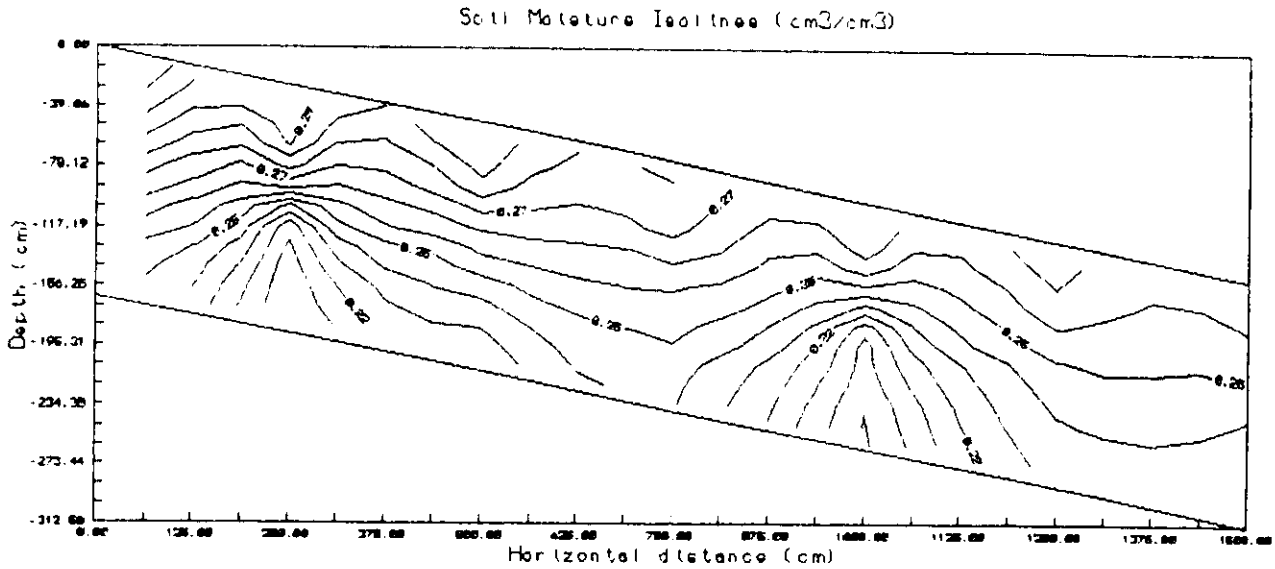

Figure 13. Soil water content isolines in a rubber-tree plantation (23/8/89).

REFERENCES

Caranahan, B.; Luther H.A.; Wilkes, J.O. **Applied numerical methods.** New York, John Willey, 1969, 604 p.

Couchat,Ph.; Carre, C.; Marcesse, J.; Leho, J. **The measurement of thermal neutron constants of the soil: application to the calibration of neutron moisture and to the pedological study of soil.** Nuclear Cross-sections Technology (Schrach and Bowman Eds.), 516. 1975.

Falleiros, M.C.; Ravello Sanches,A.; Souza, M.D.; Bacchi, O.O.S., Pilotto, J.E.; Reichardt, K. Soil water content measurements close to soil surface with a neutron moisture gange. **Sci. Agric.** 50(3) 418-425, 1993.

Greacen, E.L. **Soil water assesment by the neutron method.** Camberra, CSIRO, 1981,140 p.

Greminger, P.J.; Sud, Y.K.; Nielsen, D.R.; Spatian variabilityu of field measured soil water characteristics. **Soil Science Society of America Journal.**, 49(5): 1075-82, 1985.

Havercamp, R.; Vauclin, M.; Vachaud, G. Error analysis in estimating soil water content from neutron probe measurements: I. Local standpoint. **Soil Science.**, 137(2): 78-90, 1984.

IAEA. **Neutron moisture gauges.** Viena, 1970. 137 p. (Technical report series, 112).

IAEA. **Tracer manual on crops and soils.** Viena, 1976. 227 p. (Tecnical report series, 171).

IAEA. **Field soil-water properties measured through radiation techniques.** Vienna, 1984, 122 p. (TECDOC, 312).

Libardi, P.L.; Reichardt, K.; Nielsen, D.R.; Biggar, J.W., Simplidied field methods for estimating the unsaturated hydraulic conductivity. **Soil Science Society of America Journal.**, 44(1): 3-6, 1980.

METHODS OF SOIL ANALYSIS; part I - physical and mineralogical methods. 2.ed. Madison, ASA, 1986. 1188 p (Agronomy, 9).

Olgaard, P.L. Problems connected withthe use of subsssurface neutron moisture gauges and their solution. Danish Atomic Energy Comission. Rea Establishment Riso. Riso-M980 20.

Vauclin, M.; Havercamp, R.; Vachaud, G. Error analysis in estimating soil water content from neutron probe measurements: 2. Spatial standpoint. **Soil Science.**, 137(3): 141-48, 1984.

Villagra, M.M..; Matsumoto, O.M.; Bacchi, O.O.S.; Moraes, S.O.; Libardi, P.L.; Reichardt, K. Tensiometry and spatial variability in Terra Roxa Estruturada. **Revista Brasileira de Ciência do Solo, Campinas, 12(3): 205-10, 1988.**